Physicochemical investigations and electrical conductivity measurements on monocrystalline gallium sulphide

Lieth, R.M.A.

DOI:
10.6100/IR117987

Published: 01/01/1969

Document Version
Publisher's PDF, also known as Version of Record (includes final page, issue and volume numbers)

PHYSICOCHEMICAL INVESTIGATIONS AND ELECTRICAL CONDUCTIVITY MEASUREMENTS ON MONOCRYSTALLINE GALLIUM SULPHIDE

PROEFSCHRIFT

TER VERKRIJGING VAN DE GRAAD VAN DOCTOR IN DE TECHNISCHE WETENSCHAPPEN AAN DE TECHNISCHE HOGESCHOOL TE EINDHOVEN OP GEZAG VAN DE RECTOR MAGNIFICUS PROF. DR. IR. A.A.TH.M. VAN TRIER, HOOGLERAAR IN DE AFDELING DER ELEKTROTECHNIEK, VOOR EEN COMMISSIE UIT DE SENAAT TE VERDEDIGEN OP DINSDAG 14 OKTOBER 1969 DES NAMIDDAGS TE 4 UUR.

DOOR

RONALD MAURITS ANDRÉ LIETH

GEBOREN TE SEMARANG (INDONESIË)

Offset-Drukkerij Biblo 's-Hertogenbosch

DIT PROEFSCHRIFT IS GOEDGEKEURD DOOR DE PROMOTOR

PROF. DR. F. VAN DER MAESEN

Aan de nagedachtenis van mijn vader
Aan mijn moeder
Aan mijn vrouw en kinderen

CONTENTS

INTRODUCTION

In 1964 a solid state physics group was formed in the Physics Department of the Eindhoven University of Technology. One of the items of its research program was the study of the transport properties of gallium sulphide.
This compound was choosen for several reasons. Compared to the well known semiconducting II-VI compounds like ZnS and CdS and the III-V compounds GaP, GaAs, InSb, the III-VI family had received relatively less attention. Most of the work done on gallium compounds was reported by Mooser and Brebner*), their investigations had centered mainly around GaSe and GaTe.
Furthermore GaS has a layered structure with strong bonding in the layers and weak bonding between succesive layers. This suggests interesting anisotropic effects in the properties of this solid.

The investigations were started with the study of physicochemical properties. They comprise the preparation of polycrystalline material with an impurity concentration as low as possible, the investigation of phase equilibria in the system Ga-S and the stability of the compound at elevated temperatures. Techniques to grow single crystals and attempts to prepare doped crystals were further objects.

All these experiments served as a basis for further research on physical properties. For example the temperature-composition and temperature-pressure relationship are of importance for the post heat treatment of single crystals and for making electrical contacts.
Determination of the role played by defects and impurities in semiconductors starts with the ability to prepare a *pure* compound and depends on the possibility to introduce defects and well defined impurities (in controlled concentrations) into the material under investigation. Measurements of electrical properties of those *pure* and *impure* crystals makes it then possible to obtain information

*) Formerly at the Cyanamid Research Centre in Geneva.

about the influence those defects and impurities have.

The physical work discussed in this thesis comprises the influence of temperature on the dark conductivity. This was done for both *n*- and *p*-type crystals. Furthermore the influence of sample purity on the conductivity and the effects of heat treatments are observed. The effect of varying the iodine concentration, during the preparation of single crystals, on the conductivity is presented.

Chapter 1 contains a survey of the literature on GaS.
In chapter 2 the preparation of the compound in polycrystalline form and the attempts to suppress the impurity content in this material is described. Furthermore the phase relations in the system gallium-sulphur are discussed and the stability of the compound at elevated temperatures is studied.
In chapter 3 the three techniques used in crystal growth experiments are presented, and spectrochemical analyses of the monocrystalline compound both for *n*- and *p*-type, are given. Furthermore variations in crystal habit observed in the different growth techniques are discussed and the results of doping experiments are mentioned.
Chapter 4 deals with the measurements of the dark conductivity as a function of temperature, the effects of heat treatments and the influence of the iodine concentration on the conductivity. It concludes with an attempt to interprete the results with current semiconductor statistics and the presentation of a model for *n*- as well as *p*-type GaS.

Chapter 1

SURVEY OF THE LITERATURE ON GaS

Among the $A^{III}B^{VI}$ semiconducting compounds, some selenides and tellurides have received growing interest in the last few years, while the sulphides have attracted less attention. In this type of compounds component A is represented by one of the metals of the third subgroup of the periodic system, e.g. gallium, indium or thallium, while component B is one of the elements sulphur, selenium or tellurium.

Common to most of these divalent chalcogenides, indicated as the III-VI family, is the distinctive layered structure of their crystals. Between the fourfold layers the distance is larger than within such a multiple layer. As a result there is a difference between bond strength in the layers and between the layers.

Owing to considerable research efforts, which in recent years have been directed to a better understanding of the gallium compounds, a great deal of experimental data, mainly on the selenides and tellurides has been published. Up to now only a small number of publications have dealt with gallium-sulphide.

The earliest articles report the preparation of the compound and the determination of its crystal structure. More recently literature on optical absorption and photoconductivity of the gallium chalcogenides the infrared absorption of monocrystalline gallium, indium and thallium compounds, and photoconductivity of mixed crystals of GaS and GaSe have appeared.

The preparation of GaS was studied by several investigators. Brukl and Ortner (B_1) synthesized the compound by reducing Ga_2S_3 at 800°C in a stream of hydrogen.

Klemm and Von Vogel (K_1) prepared the compound directly from the elements, using a silica reaction tube which had a shape as shown in figure (1.1.) Compartment A contained the metal, compartment B the sulphur.

The tube was sealed under vacuum and the reaction was started by heating compartment B until the whole system was filled with

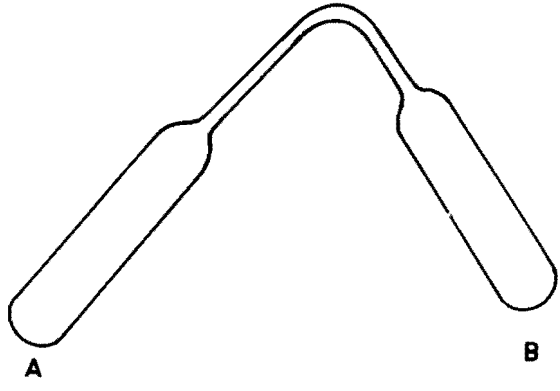

Fig. 1.1. A sketch of the silica tube as used by Klemm and Von Vogel for the preparation of GaS. Part A contained the gallium, part B the sulphur.

sulphur vapour. Thereafter compartment A was heated. Near the end of the reaction the unreacted sulphur was driven into compartment A which was cooled with water. Part A containing the reaction-product was then sealed off and reheated in a furnace for half an hour at 1100°C to complete the reaction.

Spandau and Klanberg (S_1) in their work on the thermal stabilities of the phases in the system gallium-sulphur used a modification of Klemm and Von Vogel's procedure. A silica tube filled with gallium and sulphur, and sealed under vacuum was heated for about half an hour at 1200-1250°C. Using tubes with a lenght of 200 mm and a diameter of 10 mm, the yield was about 2 grams GaS per tube.

The crystal structure was determined by Hahn and Frank (H_1), they reported a hexagonal layer structure with the following values for the lattice constants $a = 3.57$ kX and $c = 15.47$ kX. The space group is D^4_{6h}.

Fig. (1.2.) gives a schematic representation of the structure. Each layer consists of 4 sublayers in the sequence S - Ga - Ga - S, each gallium

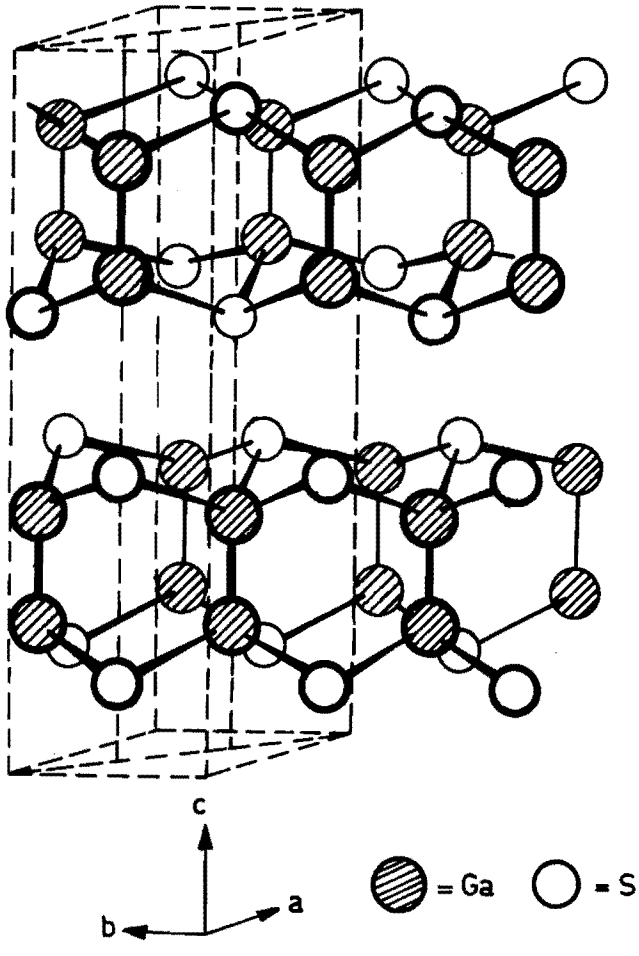

Fig. 1.2. Schematic representation of the crystal structure of GaS.

atom being surrounded by one gallium and three sulphur atoms*) in such a way that the Ga - Ga bonds are parallel to the *c*-axis.
Between the four fold layers the distance is of the order of 3 kX, the Ga - Ga and Ga - S distances in such a multiple layer are 2.46 and 2.34 kX respectively.

*) For convenience we speak of "atoms"; this doesn't imply that any information is given about the chemical bond.

While fully described solid-liquid phase equilibria of the systems Ga - Te (N_1), In - Te (G_1) In - S (H_2) In - Se (S_2) and Ga - Se (P_1) could be found, there existed no report on the phase diagram of the system gallium-sulphur. Melting points of 965°C and 1250°C for the compounds GaS and Ga_2S_3 respectively, were reported by Klemm and Von Vogel (K_1), while Spandau and Klanberg (S_1) found the melting point for GaS to be 970°C.

Furthermore no reports concerning the vapour pressures of compounds like GaS and Ga_2S_3 could be found in the literature.

According to the experiments of Spandau and Klanberg (S_1), GaS started to decompose at its melting point forming Ga_4S_5, while Ga_2S_3 would start to lose sulphur above 950°C during conversion into Ga_4S_5.

The preparation of monocrystalline GaS was described by Nitsche et.al. (N_2) and Hahn and Frank (H_1).

Nitsche and co-workers used iodine as a transporting agent in growing GaS single crystals in closed evacuated silica ampoules. The ampoule containing the polycrystalline GaS and some iodine is heated in a temperature gradient, the temperatures at the ends of the ampoules being 930°-850°C respectively.

The iodine forms a volatile compound with the metal; this compound together with the sulphur diffuses to the coolest part of the tube. Here GaS is formed again and is deposited in the form of monocrystalline plates on the tube wall.

Hahn and Frank in their structure work on GaS made use of single crystals of the solid which had grown in a sublimation process. An evacuated silica tube containing polycrystalline GaS was placed in a temperature gradient with the high and the low temperature being 950 and 750°C respectively. This resulted in a monocrystalline product partly consisting of hexagonal columns, partly of thin platelets.

While detailed reports on the absorption and photoconductivity of GaSe and GaTe and to a lesser extend of GaS can be presented, almost no literature is available on the dark resistivity of GaS as a function of temperature.

Reports on the optical absorption and photoconductivity of the gallium chalcogenides are given by Brebner and Fischer (B_2), by Brebner (B_3) by Ismailov and co-workers (I_1) and Gross and co-workers (G_2) while Akhundov and Kerimova (A_1) studied the infrared absorption of GaS, GaSe, InSe and TlSe single crystals. Reflection measurements have been performed by Nizametdinova (N_3) and Akhundov and co-workers (A_2). Photoconductivity and photo Hall-effect investigations on gallium sulphide single crystals were reported by Kipperman and van der Leeden (K_2) of our laboratory.

Photoconductivity characteristics of solid solutions of GaSe and GaS for proportions of GaS between 10% and 50% were investigated by Bube and Lind (B_4) while the optical absorption of a series of mixed crystals of the system $GaS_{1-x}Se$ at low temperature was studied by Brebner (B_5).

TABLE 1-I
Some properties of GaS, GaSe and GaTe

	GaS	GaSe	GaTe
colour	greenish-yellow (K_1)	red-brown (K_1)	blue (K_1)
structure	hexagonal (four) fold) layer (H_1) a = 3.57 kX c = 15.40 kX	hexagonal (four fold) layer (H_1) a = 3.75 kX c = 15.88 kX and rhombohedral (S_3) a = 3.73 kX c = 23.86 kX	monoclinic layer type (H_3) a = 12.7 kX b = 4.0 kX c = 14.99 kX β = 103.9°
melting-point	962° ± 4°C (L_1)	960° ± 10°C (K_1)	824° ± 2°C (K_1)
bandgap	~ 2.7 eV (K_3)	2.0 eV (K_3)	1.65 eV (B_6)

The conductivity as a function of temperatures of GaS is very briefly mentioned in the work of Fischer and Brebner (F_1).
Ismailov and co-workers (I_1) report a resistivity of about $10^{10}\,\Omega$ cm for *p*-type GaS samples. Rustamov and co-workers (R_1) who studied mixed crystals in the system GaS-GaSe, report a conductivity for *p*-type GaS of about $2.10^{-6}\,\Omega^{-1}\text{cm}^{-1}$ at about 300 K, which value decreases when heated to 373 K, to a value of $1.2.10^{-6}\,\Omega^{-1}\,\text{cm}^{-1}$.

This survey is concluded with a comparative presentation of some properties of the three gallium compounds.
In table 1-I the colour, the structure type, the melting point and the bandgap are given for GaS, GaSe and GaTe.

Chapter 2

PHYSICOCHEMICAL PROPERTIES OF GaS

In this chapter attention is paid to the preparation of the solid and the determination of the phase relations. A study of the equilibrium between the solid and vapour phase is presented, the equilibrium constant is calculated and the behaviour of the compound at elevated temperature is described.

2.1. Preparation of polycrystalline GaS

In the synthesizing process generally used, gallium sulphide is formed from the elements, in a closed silica container, by heating the metal in a sulphur atmosphere*).

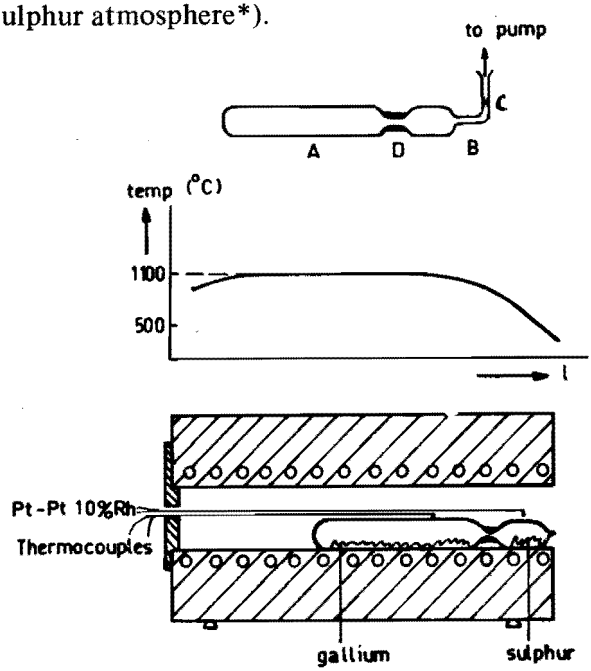

Fig. 2.1. The two-compartment silica reaction tube and the electrical furnace with the temperature gradient as used in the synthesis of GaS.

*) The gallium and sulphur (purity 99.999°/o) were obtained from Johnson Matthey and Co, Ltd. The silica is Pursil 453 from Quartz et Silice, France. Spectrochemical data are given in table 2-I and 2-II.

The silica container used as reaction tube has a shape as shown in fig. 2.1. The sections A and B are connected by a narrow tube D, part A and part B are filled with gallium and sulphur respectivily and the whole system, after being sealed off at C under vacuum (10^{-3} mm Hg), is heated in a horizontal electrical furnace.

The part containing the metal is brought to 1100°C, while the sulphur is kept at about 600°C. After about 16 hours the reaction has ended. In this procedure which is a slight modification of the technique used by Klemm and Von Vogel (K_1), the metal is in direct contact with the tube wall. At the elevated temperatures used in the reaction, the liquid gallium reacts with the silica according to the reaction:

$$4\,Ga_{(l)} + SiO_{2\,(s)} \rightleftarrows 2\,Ga_2O_{(g)} + Si, \qquad (2.1)$$

forming the volatile suboxide Ga_2O. The silicon produced in this reaction contaminates the metal, giving rise to a high Si content in the compound (C_1).

The contamination of gallium by silicon is shown in column 5 of table 2-I. Here the spectrographic analysis of gallium, which has been heated at 1000°C for about half an hour in a silica tube, is presented.

It can be seen from equation (2.1) that a decrease in the Ga_2O vapour pressure will cause a shift of the equilibrium to the right with a corresponding increase in the silicon activity.

This effect can be produced by transport of the Ga_2O vapour away from the hot zone. An immediate consequence is that more silicon is able to dissolve into the liquid gallium.

On the other hand an increase of the Ga_2O vapour pressure in the hot zone, will shift the equilibrium to the left which amounts to a suppression of the silicon content in the gallium. The use of a gallium compartment, in the reaction tube, with a volume as small as possible is therefore important. Two other facts that will help to reduce the diffusion of the oxide to a colder place in the reaction tube are the presence of sulphur vapour during the synthesis of GaS and the use of a narrow connection tube between the gallium and the sulphur compartments.

Spectrochemical analyses have furthermore proved that impurities were introduced in the different steps required in handling the metal ingots prior to the reaction process.

In a later stage of our work the gallium became commercially available in the form of small pellets. *) This reduced the number of manipulations required to obtain the metal in the desired dimension. Spectrographic analysis of this gallium is given in column 4 of table 2-I.

Considering these facts, our attempts to suppress the impurity content in the polycrystalline material resulted in an alteration of the synthesis described above.

A segmented tube of the form shown in figure 2.2 containing an alumina boat**) was used and care was taken to minimize section A.

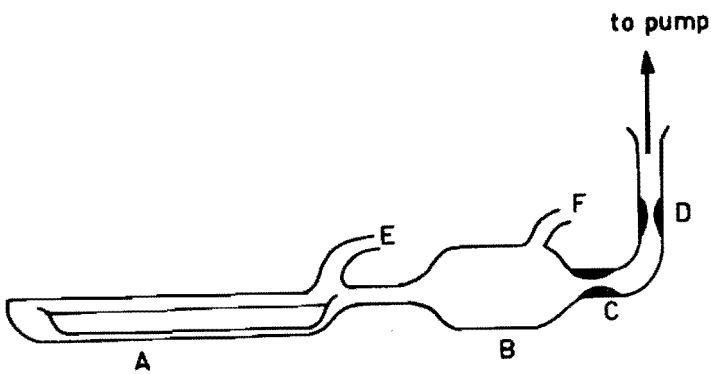

Fig. 2.2. A sketch of the modified silica reaction tube with an Al_2O_3 boat

Tube and boat are cleaned, thereafter etched in a HNO_3 - HF (3 :1) solution and carefully rinsed. To remove all traces of acid, tube and boat are repeatedly boiled in highly purified water (specific resistivity 15 M Ω cm).

The whole system is heat treated for about one hour at 1000°C in vacuo, (10^{-4} mm Hg) and vacuum is maintained while the system is cooled. The breakseal at E is opened and the boat filled with gallium

*) From Alusuisse Zurich (99.9999°/o)
**) Purox boat, 99.7°/o Al_2O_3 - from Morganite Refractory Ltd. England

which has been etched briefly in a HNO_3 - HF (1 : 1) solution prior to filling. E is then resealed and a second vacuum heat treatment at 1000°C is given in order to remove impurities adsorbed during the resealing of E. Again the system is cooled in vacuo.
Part B is then filled with sulphur using the breakseal at F which is thereafter sealed off again. When a vacuum of 10^{-4} mm Hg is reached the system is sealed off, first at D and then at C.
The reaction tube is then heated in a horizontal furnace, and care is taken to keep the metal at about 950°C, while the sulphur is kept at 600°C. The lower temperature in the gallium section prevents the reaction product from being thrown out of the boat by the heat of the reaction.

The reaction is completed in about 20 hours. Care is taken not to touch the silica parts with bare hands after completing the cleaning procedure. Perspex tweezers made in our laboratory are used when handling the Al_2O_3 boat and the metal.

Spectrochemical analyses of material obtained with these precautions*) show a decrease in the content of both silicon and sodium as compared to the earlier method, see columns 6 and 7 of table 2-I, while the aluminum and iron concentrations have increased by using a Al_2O_3 boat.
The silicon content is inhomogeneous which is explained by the inclusion of small pieces of quartz. When an ampoule is opened, small pieces of quartz are scattered into the tube. This can only be seen with microscopic examination of the surface of the crystals. Normally they escape attention and can effect the analyses.

The quantity of impurities in the Pursil type silica as stated by the manufacturer is presented in table 2-II.

---

*) The spectrochemical data presented are an average of six measurements.

Table 2-1

Spectrochemical analyses of gallium, sulphur and gallium sulphide*) (in weight ppm).

1	2	3	4	5	6	7
type of foreign atom	gallium (J.M.) 99.999°/o (ingots)	sulphur (J.M.) 99.999°/o (powder)	gallium (Alu) 99.9999°/o (small pellets)	gallium heated in SiO_2 #)	GaS prepared without boat	GaS prepared in a boat
Si	N.D.	3.10^{-1}	$\leqslant 4.10^{-2}$	4.10^{3}	8.10^{2}**)	10^{2}**)
Na	N.D.	10^{-2}	N.D.	-	2.10^{2}	N.D. (7)‡)
Fe	N.D.	5.10^{-1}	$\leqslant 2.10^{-2}$	N.D.	5	30
Al	N.D.	10^{-1}	$\leqslant .8.10^{-2}$	6	3	4.10^{2}
Cu	< 1	3.10^{-2}	N.D.	6.10^{-1}	20	8.10^{-1}
Pb	1	N.D.	N.D.	10^{3}	3	N.D.
Sn	N.D.	N.D.	N.D.	8.10^{2}	N.D.	N.D.
Mg	< 1	10^{-1}	$\leqslant 7.10^{-2}$	20	10	40

*) Tanks are due to Dr. N.W.H. Addink of the Philips Laboraties, Eindhoven.

**) Inhomogeneous due to the inclusion of small pieces of quartz. Lowest values are presented, highest values are about 10^2 times as high.

‡) Thanks are due to Dr. H.A.Das of R.C.N. Petten for the neutron activation analysis of the sodium content.

#) The gallium sample was heated in an evacuated silica tube for 30 minutes at 1000°C.

(J.M.) - Johnson Matthey and Co Ltd., England (Alu) - Alusuisse Zurich, Switzerland. N.D. = Not Detectable.

Table 2-II
Spectrochemical analysis of Pursil 453 type quartz tube (weight ppm).

Na	K	Li	Ca	Fe	Al	Ti
4	4	3	10	2	50	2

2.2. The *p*-T-X-diagram of the system Ga-S

2.2.1. Temperature-composition relation

To obtain the phase relations as a function of temperature and composition, thermal analyses were carried out on samples in closed vitreous silica tubes, with an axial thermo-couple well, see fig. 2.3. The silica tubes were filled as full as possible with the substance under investigation, evacuated and sealed off.
As the equilibrium sulphur pressures at the temperatures involved are low, as will be discussed in this chapter, the uncertainties introduced by evaporation of the sulphur from the melt are negligeable.
The samples used in our experiments, mixtures of gallium and sulphur of known composition, were heated for several hours in a vertical furnace, see fig. 2.4.

Mixtures with a sulphur content up to 50 at $^{o}/_{o}$ were heated to temperatures of 1100°C, while those with a higher sulphur content were heated up to 1300°C. Thereafter cooling curves as functions of time t were taken, the freezing points being shown by a change in the slope, or by a horizontal portion of the time-temperature curve (H_4). In order to get an indication of the form of the diagram, in the first series of cooling experiments the samples were cooled from 1100° and 1300°C respectively. This was repeated several times for every sample and with the information gained a second series of cooling and heating cycles was made on the mixtures. Each sample was therefore maintained for serveral hours at a few degrees above its liquidus temperature before it was cooled. The cooling rate was 10°C/min. Before heating curves were taken the sample was held for a time at a temperature just below the solidus.

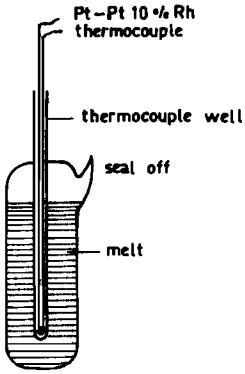

Fig. 2.3. The silica container used in the determination of the T- X diagram

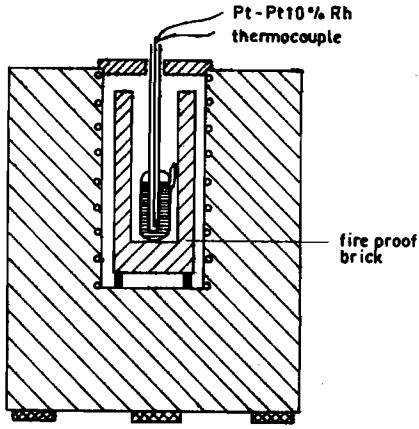

Fig. 2.4. The vertical electrical furnace used for heating and cooling of the various Ga-S mixtures. A ceramic tube is used to ensure a constant temperature over the whole length of the container.

These measurements were repeated until a difference of less than 2.5°C was obtained between the thermal arrests of cooling and heating curves of each mixtures. No supercooling occured during these experiments. Calibration of the Pt – Pt 10°/o Rh. thermocouples was carried out under identical experimental conditions by cooling curves taken on pure silver and pure sodium chloride.

In table 2-III the data found in our experiments are collected together with the colours of the various mixtures. Figure 2.5 represents, the temperature-composition diagram of the system gallium-sulphur, as composed from our results, and those of (K_1), (B_1) and (S_1).

Two maxima are found in the *T-X*-diagram. The first one occurs at the composition of GaS at 962° ± 2°C which is in good agreement with the value given by Klemm and von Vogel (K_1). The second maximum is found at the composition of Ga_2S_3 at 1090° ± 2°C and is in disagreement with Klemm and Von Vogel's work. The majority of the Ga_2S_3 exhibited a dark red colour. Occasionally a batch was ivory coloured with a mother of pearl shine on its outer surface. In the literature Ga_2S_3 is reported to be ivory coloured or white (K_1, S_1).

Debye-Scherrer photographs showed no difference between these differenly coloured substances, but on the other hand thermal analyses revealed a difference in the melting point.

Table 2-III

Melting points in the system gallium-sulphur

sulphur content, at. °/o	sample appearance	1st thermal arrest, °C	2nd thermal arrest, °C	3rd thermal arrest, °C
10	dark green with metallic Ga	959	-	-
33,5	dark green with metallic Ga	958	-	-
45	dark green with metallic Ga	958	-	-
47	dark green with less Ga	958	-	-
47.5	dark green with less Ga	958	-	-
48.5	dark green with less Ga	958	-	-
50	greenish-yellow	962	-	-
51.5	greenish-yellow	953	900	-
52	yellow	947	898	-
53.5	yellow	922	902	-
55.5	canary-yellow	900	-	-
56	canary-yellow	941	899	833
57	changing	977	896	836
58	to yellow	1007	892	828
59	red	1055	886	828
60	dark red	1090	-	-
"60"	ivory colored	1088	985	-
63	yellow-white	1080	989	-
~ 65	white	1085	980	-
99.5		119	-	-

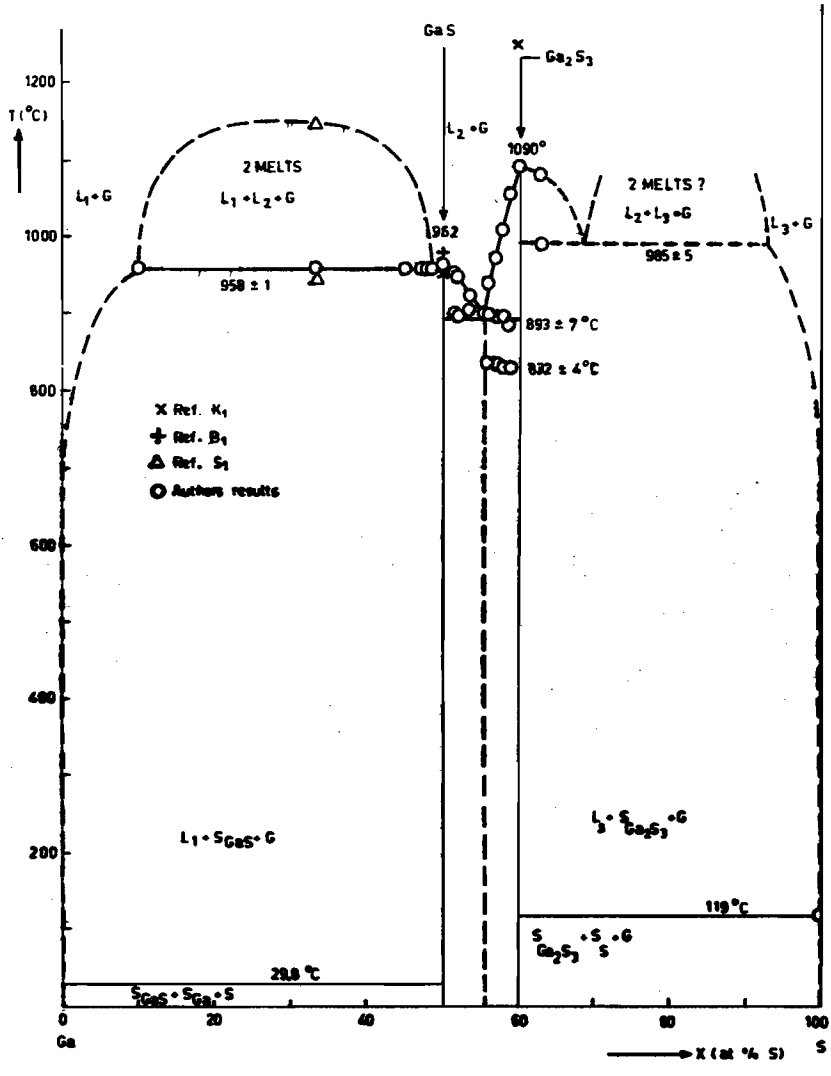

Fig. 2.5. The temperature-composition projection of the system Ga-S. (X); results of Klemm and Von Vogel, (+); results of Bruki and Ortner, (Δ); results of Spandau and Klanberg, (O); our results.

Compared with the yellow and white substances, which contain respectively 63 and ~ 65 at. °/o S, we therefore consider the ivory coloured compound with "60" at. °/o S to be sulphur-rich Ga_2S_3.

The compounds GaS and Ga_2S_3 melt at temperatures lying considerably above the melting points of the components.

On the gallium-rich side, near pure Ga, no thermal arrest above the

melting point of Ga could be detected. The first detectable melting point was at a sulphur content of 10 at. °/o. Between about 10 and 48 at. °/o S, the monotectic at 958°C indicated the existence of a range of liquid immiscibility, in good agreement with the work of Spandau and Klanberg (S_1). Analogous regions of liquid immiscibility are reported in the system Ga-Te (N_1), In-Te (G_1), In-S (H_2), In-Se (S_2) and Sn-S (A_3) and in comparing these systems with our work it is reasonable to suppose that the composition of the eutectic point on the gallium rich side must be very close to that of pure gallium.

Between GaS and Ga_2S_3 there is an eutectic point at 893°±7°C at a composition of about 55 at. °/o. S *) The effects found at 832° ± 4°C indicate the possibility of a phase transition in the solid state.

On the sulphur rich side of the diagram thermal analyses could not be carried out on samples with a sulphur content exceeding 65 at. °/o. Efforts to synthesize small samples containing more than 65 at. °/o S in large sealed quartz tubes at temperatures around 1200°C, always resulted in a mixture of Ga_2S_3 and free sulphur, which would have too high a pressure for the silica tubes used in the thermal analyses. Analogous to the systems Sn-S (A_3) and Ga-Se (P_1), a liquid immiscibility range between about 65 and 90 at. °/o S is assumed and the eutectic point on the sulphur rich side is supposed to lie close to the composition of pure sulphur.

2.2.2. Pressure-temperature relation

To obtain the phase relations as a function of pressure and temperature, the following method was used:

Mixtures of gallium and sulphur with known composition were heated with hydrogen gas, in sealed silica tubes, at various temperatures. At the temperature involved, equilibrium is attained according to the equation.

$$H_2 + 1/2\ S_2 \rightleftarrows H_2S, \qquad (2.2)$$

*) X-Ray diffraction analyses of samples with 55 at. °/o S showed lines characteristic for GaS and for Ga_2S_3 and there was no indication of the existence of a compound Ga_4S_5.

in which the sulphur pressure is the equilibrium pressure over the mixture.

When the tube is opened after a few hours, the H_2S/H_2 mixture streams into a gas volumeter filled with a sodium hydroxide solution (J_1). The volume of unreacted hydrogen can be read off and the amount of H_2S formed can be determined by iodometric titration. This procedure enables us to find the ratio p_{H_2S}/p_{H_2} under equilibrium conditions. Since the values of the equilibrium constant.

$$K_{H_2S} = \frac{p_{H_2S}}{p_{H_2} \quad p_{S_2}^{1/2}} \qquad (2.3)$$

at the various temperatures can be found in literature (R_2), the sulphur pressures can be calculated using (2.3.)

The silica tube system used in the experiments is shown schematically in fig. 2.6:

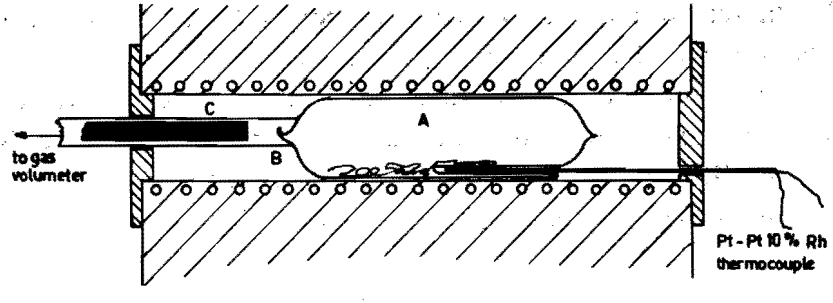

Fig. 2.6. The tube system for the determination of the partial sulphur pressure, p_{S_2}, above GaS. (A) = the reaction chamber, (B) = the breakseal, (C) = the ceramic rod.

The reaction chamber A is connected to a volumeter by a narrow tube. At this end, chamber A is equipped with a breakseal B. This can be broken by pushing a ceramic rod C against it through the narrow tube.

The furnace used was monitored by a Pt-Pt 10% Rh. thermocouple situated as shown. It could be kept constant within 3°C of the desired temperature, and had a large region where the temperature was constant. Care was taken to have A situated in this region of constant temperature. In table 2-IV the values of the sulphur pressures of

various Ga-S samples as determined by this technique are listed. Every value is an average of at least two determinations.

Some remarks about the inaccurary of the results can be made. In calculating the partial sulphur vapour pressure as a function of temperature use is made of the ratio p_{H_2S}/p_{H_2}. The inaccuracy of the titration technique used amounts to a value of 2°/o.The absolute error in the log p_{S_2} is of the order of 0,01. On account of other factors which are expected to have influence on the experiments, (such as fluctuations in the furnace temperature, and incomplete absorption of the H_2S in the NaOH), it seems reasonable to estimate the magnitude of the total error as being 0.05. The furnace can be kept constant within 3° of the desired temperature, the order of magnitude of this error at a temperature of 1000 K is 0.003 times the unit on the temperature scale.

The results are presented as a plot of log p_{S_2} versus $10^3/T$ in fig. 2.7. The sulphur pressures at the melting points of the various mixtures in the system Ga-S are presented by the curve CDF.

The vapour pressure of pure sulphur and pure gallium, the values of which are taken from literature (L_2, C_2), are shown by the lines AB and HK. The values of pure gallium are translated into sulphur pressures by means of the relation (see section 2.3)

$$K_{GaS} = p_{Ga}^2 \cdot p_{S_2}$$

The vapour pressure values of samples with a sulphur content of 50 at.°/o were determined at temperatures ranging from 798° to 927°C. The value of p_{S_2} at the melting point was obtained from these values by graphic extrapolation. These points lie on the line FG.

For samples having compositions between 50 and 55 at.°/o S the values of the partial sulphur pressure all fall along a common line; at temperatures below 900 this is represented by line DE, above 900°C these points lie on the three phase line FD. Here the sulphur vapour pressure is in equilibrium with solid GaS and liquid L_2.

For mixtures having a sulphur content which exceeds 55 at.°/o,

TABLE 2-IV

Partial sulphur vapour pressures of mixtures in the system gallium-sulphur

sulphur content (at. ^{o}/o)	temperature (^{o}C)	p_{S_2} *) (mmHg)	
45	856	$7.9.10^{-6}$	situated on line FG
50	798	$6.4.10^{-7}$	" " " "
"	810	$1.3.10^{-6}$	" " " "
"	819	$1.8.10^{-6}$	" " " "
"	910	$4.3.10^{-5}$	" " " "
"	927	$1.2.10^{-4}$	" " " "
50	962	$2.2.10^{-4}$	value found by extrapolation
52	782	$1.1.10^{-5}$	lies on line (DE)
"	877	$1.4.10^{-4}$	" " " "
"	905	$2.1.10^{-4}$	" " " "
"	949	$2.3.10^{-4}$	" " " (FD)
53	737	$3.9.10^{-6}$	" " " (DE)
"	802	$2.1.10^{-5}$	" " " "
"	926	$2.2.10^{-4}$	" " " (FD)
"	931	$2.4.10^{-4}$	" " " "
55	767	$7.1.10^{-6}$	" " " (DE)
"	787	$1.4.10^{-5}$	" " " "
"	889	$1.7.10^{-4}$	" " " "
"	897	$1.8.10^{-4}$	" " " "
55	906	$2.6.10^{-4}$	value found by extrapolation
56.5	952	$1.6.10^{-3}$	lies on line CD
57	980	$4.0.10^{-3}$	" " " "
58.5	1035	$4.9.10^{-2}$	" " " "
60	1090	1.8.	" " " "

*) 1 International atmosphere (760 mmHg) = 1.013 bar = $1.013.10^{5}$ N/m^{2} so that 1 mmHg = 133 N/m^{2}.

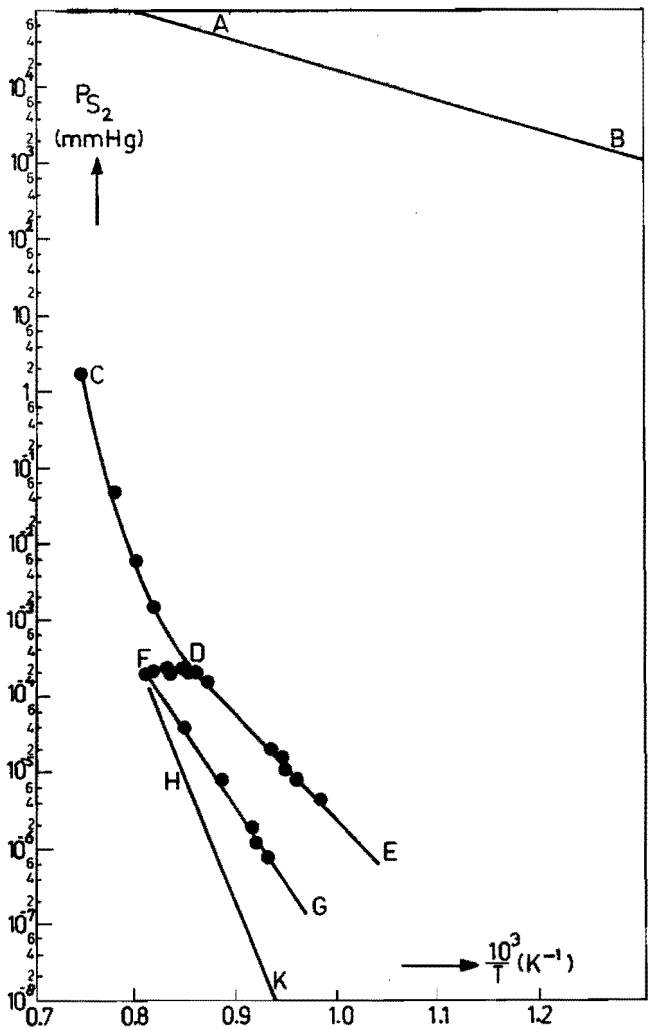

Fig. 2.7. The log p_{S_2} versus $10^3/T$ diagram of the system Ga-S. The line CDF gives the p_{S_2} at the melting point, line FG gives the pressure above solid GaS and DE the pressure above solid sulphur-rich GaS. AB gives the p_{S_2} of pure sulphur, HK gives the "p_{S_2}" of pure gallium (namely the vapour pressure of pure Ga translated into a sulphur pressure).

the values of p_{S_2} at the melting points form the three phase line CD, here the vapour is in equilibrium with solid Ga_2S_3 and liquid L_2.

The three phase line for gallium rich GaS is identical with the

line FG. For mixtures with a sulphur content of more than 60 at.^{o}/o no p_{S_2} values have been measured. For compositions above~ 65 at. ^{o}/o S, it becomes extremely difficult to measure the sulphur pressures of the three phase line on a point by point basis.

The line DE, which starts from the quadruple point D, (S_{GaS} + $S_{Ga_2S_3}$ + L_2 + G) being the eutecticum between GaS and Ga_2S_3, thus represents the sulphur vapour pressure as a function of temperature, over solid GaS which is brought to the sulphur rich side of its existence region. Line FG represents the p_{S_2} over solid GaS which is brought to the limit of its existence region on the gallium rich side. This means that the homogeneity range for GaS can not extend beyond these limits.

2.2.3. Pressure-composition relation

From the data of the *T-X* projection and the p_{S_2}-*T* projection, a p_{S_2}-*X* projection of the three-phase lines S_{GaS} + L + G and, $S_{Ga_2S_3}$ + L + G can be deduced, see fig. 2.8.
This diagram shows the increase of the sulphur vapour pressure of substances with a sulphur content between 0-and about 10 at.^{o}/o and between 50- and 60 at.^{o}/o.
Along with the assumption of a second range of liquid immiscibility for substances with a sulphur content > 65 at.^{o}/o in the *T-X* projection, one must assume a continuous rise in the sulphur pressure beyond Ga_2S_3 with increasing sulphur content until a second liquid phase appears, being the liquid immiscibility region. From here on the p_{S_2} remains constant with increasing sulphur content until the Ga_2S_3-rich liquid (L_2 in the *T-X* diagram) has disappeared. Adding still more sulphur will lower the melting point and also the vapour pressure until at 100 at.^{o}/o S the melting point will be 119^{o}C and the pressure around 3.10^{-2} mm.

2.3. Equilibrium between solid and vapour

When GaS is heated at a temperature below its melting point, an equilibrium is established between solid GaS and gallium, sulphur and

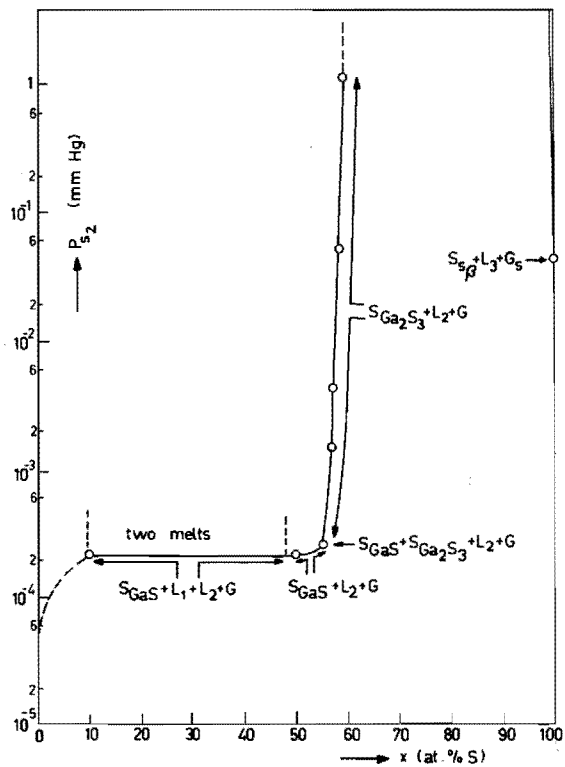

Fig. 2.8. The log p_{S_2} versus composition projection of the system Ga-S, S_β is monoclinic sulphur.

gallium sulphide in the vapour phase. This is represented by the equation

$$2\,GaS_{(s)} \rightleftharpoons 2\,GaS_{(g)} \rightleftharpoons 2\,Ga_{(g)} + S_{2(g)}. \qquad (2.4)$$

At a given temperature definite pressures p_{Ga}, p_{S_2} *and* p_{GaS} are formed, the p_{GaS} being considerably higher than p_{Ga} and p_{S_2}, as will be described in section 2.4.

The partial pressures of the components are not independent but coupled by the equilibrium constant of reaction (2.4) i.e.

$$K_{GaS} = p_{Ga}^2 \cdot p_{S_2} \quad , \tag{2.5}$$

where the activity of GaS in solid gallium sulphide is taken to be equal to unity.
The total pressure over solid GaS is equal to the sum of the partial pressures

$$P_{tot} = p_{Ga} + p_{S_2} + p_{GaS} \quad , \tag{2.6}$$

and this total pressure will change at a defenite temperature if one of the components is varied. The only constraint on the system is equation (2.5) i.e. the product of the partial pressures of gallium and sulphur must remain constant.

At any temperature there exists a minimum for the total pressure $(P_{tot})_{min}$, and this value corresponds to the condition that

$$\frac{\partial P}{\partial p_{Ga}} = \frac{\partial P}{\partial p_{S_2}} = 0 . \tag{2.7}$$

Substitution of relation (2.5) into (2.6) and using (2.7) leads to the relations:

$$p_{Ga} = 2p_{S_2} = 2^{1/3} K_{GaS}^{1/3} \quad , \tag{2.8}$$

and

$$(P_{tot})_{min} = (3/2) \cdot 2^{1/3} K_{GaS}^{1/3} \quad . \tag{2.9}$$

which show that the gasphase in the minimum has the composition of the compound.
The minimum vapour pressure is important because it plays a role under many experimental conditions. When the solid is heated under vacuum in a closed container, for example, or in a current of inert gas,

a situation corresponding to the minimum vapour pressure can arise if the sublimation rate of the solid is high in comparison to the transport rate in the atmosphere.
Under such experimental conditions GaS has a p_{S_2} (at $(P_{tot})_{min}$) and since heating of the solid does not show decomposition effects, we assume this p_{S_2} (min) to be equal to the partial sulphur pressure over solid GaS (see fig. 2.7.) This gives us the following equation

$$\log p_{S_2} \text{ (at } P_{tot})_{min} = -\frac{20773}{T} + 10.32. \qquad (2.10)$$

Here the pressure is expressed in atm.

Using (2.8) we arrive at the expression

$$\log K_{GaS} = -\frac{62319}{T} + 31.56 \qquad (2.11)$$

As a check, K_{GaS} was calculated from thermodynamic data by applying the relation

$$-RT \ln K_{GaS} = \triangle G^{O}, \qquad (2.12)$$

where $\triangle G^{O}$ represents the standard Gibbs free energy change of the reaction.
Use is now made of the relation:

$$\triangle G^{O}_{T} = \triangle H^{O}_{298} + \int_{298}^{T} \triangle C_p \, dT - T \triangle S^{O}_{298} - T \int_{298}^{T} \triangle C_p/T \, dT, \qquad (2.13)$$

and enthalphy, entropy and heat capacity values given in literature

(K_4, S_4, L_3) are inserted*)

For $\triangle H^o_{298}$ a value of 253800 cal/mole is obtained and for $\triangle S^o_{298}$ a value of 102.73 cal/degr. mole.

Heat capacity data for gaseous gallium and diatomic sulphur are from Stull and Sinke (S_4), while for solid GaS a C_p value of 12 cal/degr. mole is assumed, according to the Neumann-Kopp rule (S_5). This leads to a $\triangle C_p$ value of 4 cal/degr. mole.

The standard Gibbs free energy change at the temperature T can now be written as

$$\triangle G^o_T = 254992 - 106.76\ T + 4\ T \ln \frac{T}{298} \text{ (cal/mole)} \qquad (2.14)$$

Neglecting the contribution of the logarithmic term in (2.14), relation (2.12) can be expressed in the form

$$\log K_{GaS} = -\frac{55796}{T} + 23.36. \qquad (2.15)$$

The difference between the expressions given in (2.11) and in (2.15) can be understood when the following is considered.

Relation (2.11) results from the assumption that p_{S_2} (min) equals the partial sulphur pressure over solid GaS as found with the H_2/H_2S method. This is not necessarily so; it is possible that p_{S_2} (min) has a slope that differs from the assumed one. Furthermore, in relation (2.15), use is made of an estimated entropy value for solid GaS, since no value could be found in literature.

For experimental work, the expression given in (2.11) has to be used. If 2.15 is used - for example to calculate p_{S_2} (min) as a function of temperature - a line is found which lies outside the homogeneity range of GaS, namely on the gallium rich side. This would mean that GaS would decompose on heating.

---

*) As no values for the entropy of the compound GaS could be found, an estimated value of 16 cal/degree, based on the theory of Latimer was used.

2.4. The vapour pressure of GaS

In the expression for P_{total}, see equation (2.6.) the partial pressure of the undissociated molecule p_{GaS} also occurs.
By means of a dynamic method of vapour pressure determinations as described by Kubaschewski (K_4), measurements of p_{GaS} at various temperatures were performed.

In this technique a steady, measured, stream of purified inert gas*) is passed over polycrystalline GaS which is kept in an open silica tube with a shape as shown in figure 2.9. The tube system is kept at a constant temperature in a horizontal furnace. The vapour from the sample is then condensed at some point down stream and the vapour pressure is calculated from the amount of sample material collected in a known time interval.

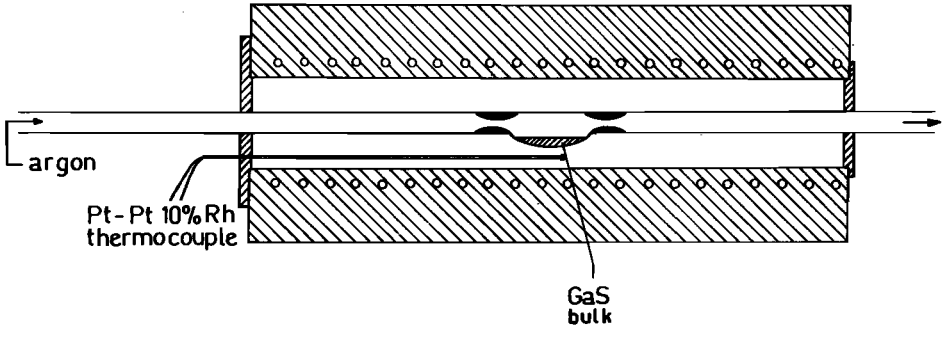

Fig. 2.9. The open tube system for the transportation of the GaS vapour.

The vapour is removed at a rate which is dependent upon the velocity of the carrier gas and upon the partial pressure of the vapour. In practice, saturation of the transporting gas is attained by using low yet finite streaming rates. However, if the velocity of the gas is reduced too much, an error can be introduced by thermodiffusion on account of the long duration of each experiment. For example this situation exists at temperatures lower than 900°C, when the amounts of transported GaS are very small, thus requiring a protracted experiment.

*) Argon, which was deoxidized over BTS pellets and dried over molecular sieves, was used as the transporting agent in these experiments.

In order to minimize counter diffusion of the vapour, constrictions were made in the silica tube on both sides of the sample section. Condensation of the vapour takes place in a cooler part of the tube system. The greenish-yellow polycrystalline material is collected and weighed at the end of each experiment, while the total volume of the carrier gas used during each experiment is measured.

Under assumption of the validity of Boyle's law, the partial pressure p_{sub} of GaS can now be calculated from the volume V_{gas} of the carrier gas at 0°C and 760 mm Hg and from the volume V_{sub} of the transported GaS by using the equation

$$p_{sub} \text{ (mm Hg)} = \frac{V_{sub} \times 760}{V_{gas} + V_{sub}} , \qquad (2.16)$$

as given by Kubaschewsky (K_4).

The results are presented in table 2-V *).
The experiments were carried out between 900° and 1100°C. As the majority of the experiments were performed with at least two different gas flow rates, the equilibrium attained must be independent of the gas rate. The results are plotted in fig. 2.10 as a log p_{GaS} versus $1/T$ diagram.

The line S G gives the vapour pressure of GaS below its melting point in the range 910°-960°. It can be represented by the equation:

$$\log p_{GaS} = - \frac{23365}{T} + 19.49. \qquad (2.17)$$

In an analogous way, the line L G giving the vapour pressure of the compound above its melting point, is represented by the equation:

$$\log p_{GaS} = - \frac{5605}{T} + 5.17. \qquad (2.18)$$

---

*) GaS is assumed to be monomeric in the vapour phase.

TABLE 2-V

Determination of the vapour pressure of GaS by the transportation method

temperature (°C)	flow rate of carrier gas (ml/min)	weight of material carried forward (mg)	volume of carriergas (litres)	vapour pressure (mm Hg)	presented by line
913	8.52	3.6	0.945	0.70	SG
	2.47	3.8	0.945	0.74	"
927	11.36	6.2	1.000	1.14	"
	4.45	4.5	0.850	1.09	"
930	4.54	5.0	0.900	1.02	"
945	6.81	9.3	0.900	1.90	"
	9.31	10.0	1.000	1.84	"
947	9.20	9.2	1.020	1.71	"
952	7.40	12.7	1.000	2.32	"
	4.82	12.2	1.000	2.25	"
960	6.21	15.0	0.770	3.59	"
	4.0	13.6	0.700	3.66	"
	10.3	15.5	0.930	3.06	"
1017	6.85	33.7	0.890	6.94	LG
	4.50	31.8	0.825	7.02	"
	8.31	36.6	0.915	7.34	"
1054	2.80	23.0	0.550	7.67	"
	5.07	33.1	0.810	7.50	"
	7.47	42.4	1.000	7.79	"
1057	4.82	4.20	0.770	9.98	"
1075	7.73	52.9	1.000	9.73	"
	4.64	38,1	0.720	9.82	"
1095	5.86	58.7	0.850	12.70	"
	6.47	68.2	0.980	12.65	"
1097	4.04	66.0	0.890	13.31	"

Comparison of p_{GaS} at the melting point of the solid with the partial sulphur pressure p_{S_2} at this temperature shows p_{GaS} to be about 10^4 times as large as p_{S_2}.

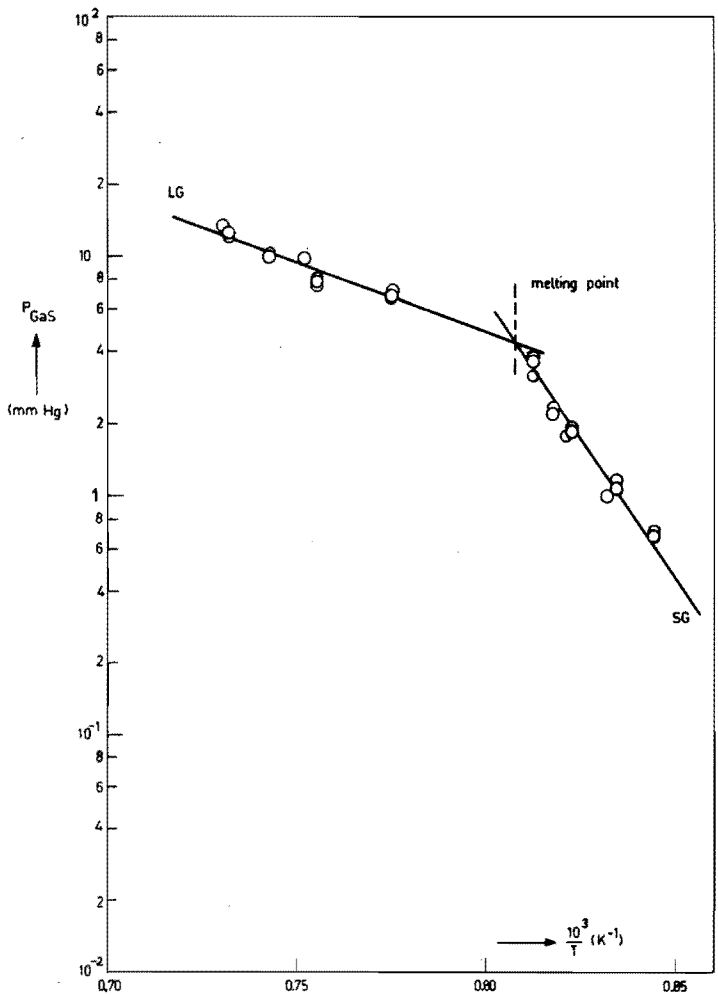

Fig. 2.10.The log p_{GaS} versus $10^3/T$ diagram. The line SG represents the equilibrium solid-vapour, while LG presents the equilibrium liquid-vapour. From the slope of SG, ΔH is found to be 107 ± 5 Kcal and $\Delta S = 89 \pm 5$ Cal, for LG this gives $\Delta H = 25 \pm 8$ Kcal and $\Delta S = 23 \pm 10$ Cal.

2.5. Stability at elevated temperatures

While the afore mentioned experiments where performed with moderate gasflow rates, preliminary experiments had shown that at higher temperatures and with higher flow rates of the carrier gas, a considerable amount of product was transported to the cooler part of the tube. This condensate exhibited different colours and looked quite like the products found in early crystal growth experiments using the sublimation technique. These results were in agreement with the work of Spandau and Klanberg (S_1) who found the same coloured product in transportation experiments exceeding 960°C. These authors assumed this condensate to be the decomposition product of GaS and proposed it to be the compound Ga_2S, inspite of the fact that their Debye-Scherrer pictures revealed a hexagonal structure almost exactly like that of GaS.

It seemed therefore important to examine the effects of heating the solid in an open as well as in a closed system.

Following the same procedure as described in the preceding section transportation experiments were performed with other bulk temperatures and other flow rates of the carrier gas. The duration of the experiments was also varied.

In all cases where high gas flow rates were combined with high temperatures, a considerable amount of condensate was found which displayed different colours. Only in one case with a moderate gas flow and performed at a temperature below the melting point of GaS was such a coloured product found, but this experiment was of a much longer duration.

In the first series of experiments, GaS was heated at 1120°C under an argon stream of 12.6 ml/min. After 1 3/4 hours the tube was cooled down, the argon flow stopped and the condensation product examined.

In region A (fig. 2.11) the cooler part of the system, a black ring could be seen. Microscopic examination showed no gallium spheres in this condensate.

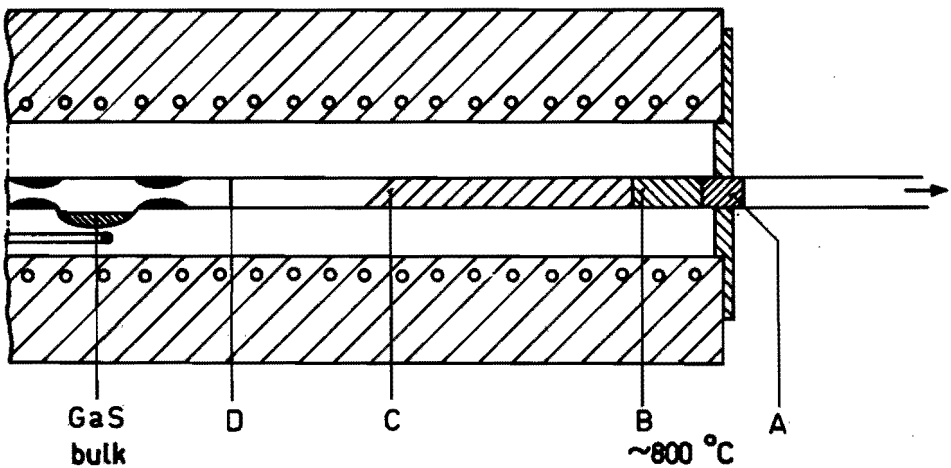

Fig. 2.11. The tube system used in the stability experiments.

In part B a dark-green plug containing small greenish-yellow hexagonal columns was seen, while region C contained small plate-like crystals. On microscopic examination gallium droplets were clearly visible and the violent reaction with bromine under water confirmed the presence of free gallium, as GaS is not reactive under these circumstances. It is therefore felt that the condensed product consits of GaS contaminated with gallium and that no compound Ga_2S exists.

In the course of the first experiment the source material had changed in colour. At the start greenish-yellow, characteristic for GaS with a very small excess of Ga, the bulk had turned more yellow.
The tube containing the condensed products was cut off at D (fig. 2.11) replaced by a clean one and the experiments repeated with the same source material. At 1120°C, with a flow rate of 23.5 ml/min, the same coloured condensate was found after 1 3/4 hour; at 900°C, with the gas flowing at a rate of 8 ml/min, no condensation product was seen even after five hours.
Repeated at 936°C, with a moderate gas flow of 6.8 ml/min, the coloured condensate was produced in four hours.
No further change in colour of the bulk material could be seen.

In the second series a mixture of GaS and gallium - having an overall composition equivalent to Ga_2S - was used as source material.

With the bulk at 900°C and the gas flowing at a rate of 10.4 ml/min. no condensate was detected after two hours. Repeating it at 1100°C with a flow rate of 15.3 ml/min the same coloured product was seen again, after two hours.
In this second series, the dark green bulk material had not changed in colour during the experiments.

The effect of heating the compound in vacuo (10^{-3} mm Hg) in a closed container is demonstrated in the last experiment.A small amount of GaS powder was placed in the middle of a long silica tube,see fig. 2.12, with a volume of 276 cm^3. The part containing the bulk was kept at 930°C, while both ends were at about 800°C. After 19 hours the heat treatment was stopped and gallium was seen in the coldest parts, denoted by A in fig. 2.11. The parts denoted by B had the yellow colour of sulphur rich GaS. On both substrates, single crystals in the form of hexagonal columns and thin ribbon-like plates had grown.

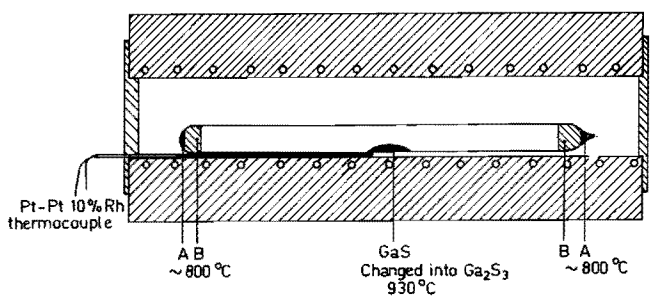

Fig. 2.12. Closed-tube system with GaS in the middle of the ampoule.

The rest of the bulk material in the middle of the tube had almost completely turned dark-red in colour except for the part in close contact with the tube wall, which had remained yellow. This means that about 90% of the bulk had changed its composition to (red) Ga_2S_3 (see table 2-III).

The results of the described experiments are listed in table 2-VI. The excess of metal on the GaS deposit is explained by the fact that GaS dissociates slightly, according to equation (2.4), at the elevated temperatures. Gallium, having above the source a partial vapour pres-

TABLE 2-VI

Determination of thermal stability by the transportation method using a carrier gas

series	number	temp. of bulk (°C)	gas rate (ml/min)	time (min)	condensation products in cooler part of tube	colour of bulk after experiment
1 greenish-yellow GaS source material	I	1120	12.6	105	black ring, dark-green plug, yellow-green columns	more yellow
more yellow GaS	II	1120	23.5	105	same products	yellow
yellow GaS	III	900	8.0	300	no condensation products to be seen	no change; yellow
	IV	936	6.8	240	same condensation product as in I and II	no change in colour, still yellow
2 GaS + Ga ($\sim$ Ga_2S) (dark green)	I	900	10.4.	120	no condensation product to be seen.	unchanged dark green
dark green	II	1100	15.3	120	same products as in series 1, I and II	unchanged dark green
3 closed container, vacuum		930		1140	free gallium and yellow GaS in both ends	turned into red Ga_2S_3

sure which is higher, but close to the equilibrium pressure of pure gallium at $\sim$ 800°C *) ,will condense near the GaS deposit in the cooler part of the system and the back reaction of the dissociation products to form GaS can be neglected at these temperatures.
On the other hand p_{S_2} above the source is lower than the equilibrium pressure of pure sulphur at 800°C **). The greater part of the sulphur in the vapour will therefore disappear in the case of an open system. In the experiment with the closed container gallium is continuously taken away from the vapour by condensation at the coldest end, and the rising partial sulphur pressure, reacting with the GaS bulk material, forms Ga_2S_3.

2.6 Conclusions

Precautions are taken during preparation of polycrystalline gallium sulphide from the elements and the spectrochemical data presented show a decrease in the concentration of Na, Si, Cu. On the other hand an increase in the amount of Fe, Al and Mg is observed which is probably due to the fact that a Al_2O_3 boat was used in the synthezation process.

From the slope if the liquidus curve in the T-X diagram, it is apparent that growth of crystals from an off-stoichiometric melt is confined to a very dilute metal-rich system. This in general does not lead to large and well formed crystals. One is therefore bound to stoichiometric mixtures when the melt growth technique is used.
The p_{S_2}-T diagram shows the low p_{S_2} values for the compound GaS and it shows that the homogeneity range of the compound lies to the sulphur rich side. On the other hand the p_{GaS} is shown to be considerably higher, which is of importance for heat treatment procedures of crystalline material; higher temperatures will cause sublimation of the crystal.

---

*) p_{Ga} above GaS at 930°C for example is $\sim 4.10^{-4}$ mm Hg, while p_{Ga} above pure gallium is $\sim 1.2.10^{-5}$ mm Hg.

**) p_{S_2} above GaS at 930°C is $\sim 2.10^{-4}$ mm Hg, while p_{S_2} above pure sulphur at 800°C is $\sim$ 54 atm.

The behaviour of GaS at elevated temperatures shows the compound to be rather stable. Transport of the vapour will show decomposition products only when the condensation temperature lies below a temperature of about 820°C.

Chapter 3

THE PREPARATION OF MONOCRYSTALLINE GaS

This chapter deals with the preparation of monocrystalline gallium sulphide by two basic methods i.e. growth from a liquid phase and growth from the vapour phase.
Furthermore the variation in crystal habit, observed for vapour grown crystals is discussed and attempts to dope GaS are described.

3.1. Crystal growth experiments

In the following three sections the techniques used in crystal growth are discussed. These are the iodine transport process, the sublimation method and the melt growth technique.

The iodine transport process is an attractive method for preparing GaS single crystals on account of the relative ease of handling, the short duration of the process and the dimensions of the obtained crystals.
Provided that the amount of iodine used is high enough, the resulting crystals will show distinctive *n*-type conductivity. Decrease of the iodine beyond a certain limit will change the type of conductivity into-*p*-type. This marked influence on the electrical properties of the solid is due to the incorporation of iodine.

A decided advantage of the two other techniques is the fact that an iodine free solid is achieved which shows *p*-type conduction. The difficulties so often encountered in the growth of crystals by direct sublimation - as in the case of III-V compounds (M_1) - is not met when working with gallium sulphide. There is no need to heat the solid above its melting point, as the vapour pressure of GaS at about 930°C is high enough to ascertain vapour phase transport to the cool end of the reaction tube. Provided that the right temperature gradient

is used, the growing crystals will not be contaminated with the free metal either, as discussed in section 2.5.

The directional freeze technique is a valuable tool because of its simplicity. The chief advantage is that monocrystalline slices, which are thicker than the crystals obtained in the vapour transport, method, can be cut from the ingot. In our experiments, the Stöber technique of directed freezing was used. It has the advantage that there is no relative motion between furnace and crucible: The fact that the temperature involved exceeds the melting point is no disadvantage either. On the other hand control of the temperature is more critical and the longer duration of the experiment enhances the possibility of diffusion of impurities through the walls of the silica vessel containing the molten compound.

3.1.1. The iodine process

It was known from the work of Nitsche et al (N_2) that crystals of gallium sulphide could be grown readily in closed reaction tubes, with iodine as an agent.
Following Schäfer (S_6), who was the first to introduce the term "chemical transport reaction", such a process can be presented in the general form

$$iA_{(s) \text{ or } (l)} + kB_{(g)} \rightleftarrows jC_{(g)} + lD_{(g)}. \qquad (3.1)$$

Transport of A takes place under certain conditions, namely that only gaseous products are formed on the righthand side of this reaction, that the reaction is reversible and that a concentration gradient is maintained. If a reaction tube containing the reactants A and B is placed in a temperature gradient with A and B at a temperature T_1, Schäfer found that crystals of A grow at a temperature T_2, which is lower, or higher than T_1, depending on whether the reaction (3.1.) is endotherm or exotherm.

In the reaction of GaS with iodine the intermediate gaseous products probably consist of sulphur and a mixture of gallium mono- di- and triiodides. This is assumed on account of the colours of the residual mass; since, when the reaction tube is cooled, the residual mass displays different colours, which according to the literature (S_7, R_3) correspond to GaI, GaI_2 and GaI_3.
Furthermore no free iodine can be detected. Therefore it is assumed that the reaction consists of the following steps.
In the hottest part of the tube the initial reaction proceeds according to

$$GaS_{(s)} + \frac{x}{2} I_{2\,(g)} \longrightarrow GaI_{x(g)} + 1/2\, S_{2(g)}\,, \qquad (3.2)$$

with x having values or 1 or 2.
These vapours move towards the cool end of the tube by diffusion where disproportionation of the mono- and diiodides takes place according to the exothermic reaction.

$$3\, GaI_{(g)} + S_{2(g)} \rightleftarrows GaI_{3(g)} + 2\, Ga_{(g)} + S_{2(g)}, \qquad (3.3)$$

or $3\, GaI_{2(g)} + 1/2\, S_{2(g)} \rightleftarrows 2\, GaI_{3(g)} + Ga_{(g)} + 1/2\, S_{2(g)}$.

Here GaS is deposited in the form of crystals according to the reaction

$$2\, Ga_{(g)} + S_{2(g)} \longrightarrow 2\, GaS,$$

and GaI_3 diffuses back to the high temperature region, where it reacts with GaS to form GaI_x.
In preliminary work on crystal growth with the iodine transport method, Heijligers (H_5) found the optimal conditions for growth to be dependent on the tube diameter and the iodine concentration used. The best results*) were obtained with quartz tubes of about 180 mm

*) With this we mean that the crystals obtained are as uniform as possible in thickness and without being intergrown. It definitely does not imply that these crystals are as large as possible. Larger but more intergrown plates are produced in tubes having diameters between 30-35 mm with a length of 180 mm.

length and 20 mm inside diameter, containing 3-6 mg iodine per cm^3 tube volume. In our experiments the following procedure was used. A tube system as shown in fig. (3.1) was used for filling the reaction-ampoule with iodine. The etched and cleaned reaction tube denoted A which is vacuum baked (10^{-4} mm Hg) prior to use, is loaded with 2 grams polycrystalline GaS, sealed to the system and evacuated again while it is gently heated with a hand torch.

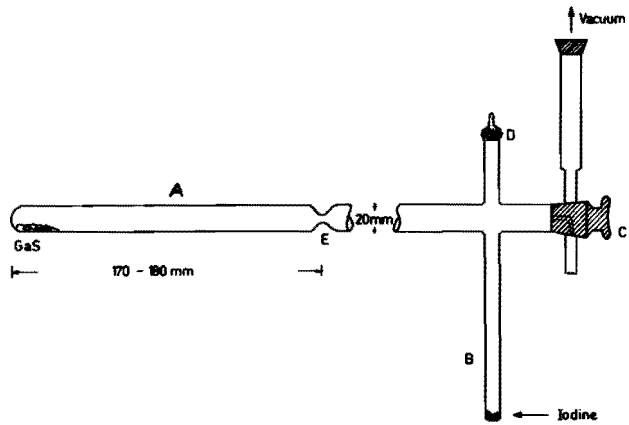

Fig. 3.1. Tube system used for filling the reaction ampoule with iodine; (A) = reaction ampoule, (B) = iodine reservoir, (C) = stopcock, (D) = stopper, (E) = seal-off.

Then when the whole system has cooled to room temperature, stop-cock C is opened, section B is loaded through stopper D with a given amount of iodine *) usually 4 mg I_2/cm^3) and the whole system is evacuated, to about 10^{-3} mm Hg. Meanwhile a Dewar flask filled with liquid air is kept around B to prevent the iodine from evaporating. Vacuum is maintained in the apparatus by turning stopcock C and the tube system can be disconnected from the pump. Cooling section A with liquid air, section B is then heated gently with a hand torch until all iodine has sublimed into section A which is subsequently sealed off at E.

*) Doubly sublimed iodine from Merck A.G. Germany.

The reaction tube A is heated in a temperature gradient in a two-zone horizontal furnace. The zones are independently heated and automatically controled, the high and low temperature being 930° and 850°C respectively, fig. (3.2).

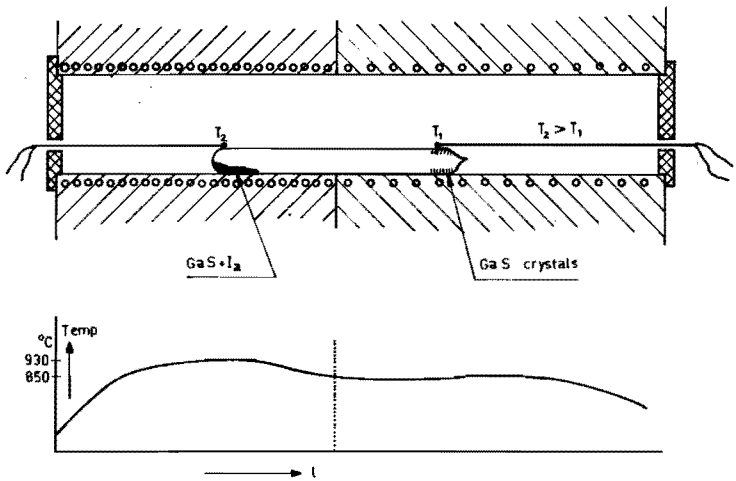

Fig. 3.2. Two-zone furnace with temperature profile for the iodine-growth process.

After about 17 hours the tube is taken out of the furnace, the hot end first. Cooling this end in water, the volatile components are forced to condense there and contamination of the crystals with the volatile gallium iodides is avoided.

The compound grows in the form of greenish-yellow plate-like crystals, with their *c*-axes normal to the plane of the plate. The largest plates are approximately 10 mm x 8 mm x 10^{-2} mm.
Decreasing the iodine concentration, a decrease in the growth rate is observed and below a certain limit the conductivity changes from *n*- to *p*-type (S_8).

In table 3-I data regarding the rate of transport in relation to the amount of iodine used in the transport process, are presented.

TABLE 3-I

Rate of transport and the amount of iodine used in the transport process
Tubes are 170 mm in length with a diameter of 20 mm
the high temperature is 930°C, the low temperature is 850°C

amount of iodine (mg/cm^3)	crystal habit	rate of transport (mg/hour)	type (S_8)
10	plates	53	*n*
6	plates	27.6	*n*
4	plates	6.3	*n*
2	plates	5.5.	*n*
1	plates	1.9	*p*
0.5	small plates	1.1	*p*
0.25	small plates and needles	1.5	*p*

The impurity content of the monocrystalline material produced with this vapour transport method is given in table 3-II. Here spectro-chemical analyses of two batches are given. Column 2 gives the result when polycrystalline GaS is used, which was prepared without an alumina boat. Column 3 shows the concentration of foreign atoms when boat grown polycrystalline material is used in the transport process.

3.1.2. The sublimation method

Since single crystals grown by the iodine transport process can suffer from the incorporation of appreciable concentrations of iodine

(S_9), other crystal growth techniques were tried.

Growth from the vapour can usually be separated into three stages: transport of the vapour to a cooler place, initial nucleation and the subsequent growth of the crystal. The vapour can be transferred in a temperature gradient and with certain precautions condenses in the form of a single crystal, or enlarges an existing single crystal seed. The initial nucleation depends on the difference in temperature between the charge and the nucleation site, which gives rise to a difference in vapour pressures. At the growth place the vapour becomes supersaturated and nucleation starts. Determination of the optimum value of the supersaturation has to be done experimentally.

The subsequent growth is to a large extent dependent on the dissipation of the heat of condensation released. Removal of the heat of crystallisation must take place in such a way that the temperature at the growing face of the crystal is not altered significantly since alteration can lead to a change in supersaturation. In so far increase of supersaturation occurs this can lead to the formation of a large number of separate nuclei and then result in a polycrystalline mass.

The following procedure was adopted in our sublimation experiments: a reaction tube with the same dimensions as those used in the iodine transport process undergoes the same procedure of cleaning, etching and vacuum baking and is subsequently filled with approximately 2 grams of polycrystalline material. The starting material used is prepared according to the description given in chapter 2.

The ampoule is then sealed off under vacuum of 10^{-4} mm Hg. In a horizontal two-section furnace with independently heated and automatically controlled sections, the powder bearing part of the ampoule is maintained at 930°C, the growth site is kept at 900°C. fig. 3.3.

The time required for a run is about 100-120 hours, which is much longer than in the iodine process. The rate of transport is about 5.5 mg/hour. However the yield of useful plates is very low, about 2-5 per ampoule. The crystals obtained are of two types; thin plates and hexagonal rods. The rods have their *c*-axes parallel to their growth axes and can measure up to 5 mm in length with a diameter of about

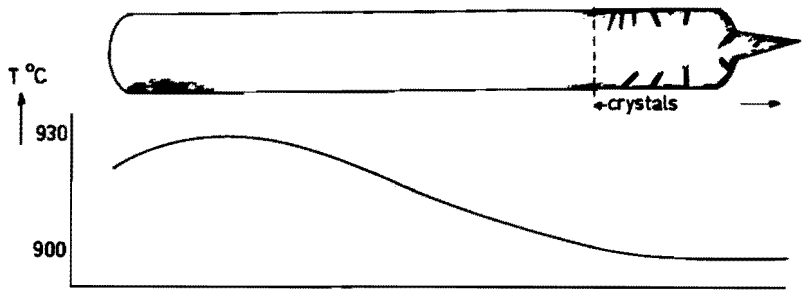

Fig. 3.3. Temperature profile during sublimation-growth process.

500-800 micron.

The majority of the plates are very thin, in the order of 2 micron, their *c*-axes are normal to the plane of the plate.

Spectrografic analyses of plates and rods are given in table 3-II, columns 4,5 and 6. Two batches are compared, rods and plates grown from GaS starting material that was prepared in an alumina boat, and plates grown from material prepared without a boat.

3.1.3. The melt growth technique

As mentioned in the introduction to this section, use is made of the technique developed by Stöber (S_{10}). The freezing plane moves through a stationary crucible, which contains the melt.

The vertical furnace is heated until the material is completely molten whereafter the temperature is decreased slowly by using a clock work driven variac to control the power. Directional freezing takes place from the bottom upwards.

For the sake of crystal perfection thermal and mechanical fluctuations must be avoided.Such fluctuations cause irregular growth.Furthermore it seems probable that the slower the growth rate the better the resulting crystals.

The main factor opposing the propagation of a nucleus is the latent heat of solidification. An embryo nucleus being at the same temperature as the melt will absorb any latent heat which tends to raise its

TABLE 3-II

Spectrochemical*) analyses of monocrystalline gallium sulphide (weight ppm)

1	2	3	4	5	6	7
impurity	grown by the iodine transport process		grown by the sublimation method			grown from the melt -
	the polycrystalline GaS was prepared without a Al_2O_3 boat	the polycrystalline GaS was prepared in a Al_2O_3 boat	the polycrystalline GaS was prepared in a Al_2O_3 boat	the polycrystalline GaS was prepared without a Al_2O_3 boat		the polycrystalline GaS was prepared in a Al_2O_3 boat
Si	6.10^2	10	6	5**)	3.10^2	50
Na	3.10^2	N.D. (15) ‡)	N.D.	N.D. (3.3) ‡)	2.10^2	4.10^3
Fe	10	10	N.D.	N.D.	20	60
Al	6	4	N.D.	N.D.	2	30
Cu	8.10^{-1}	N.D.	5	8.10^{-1}	3.10^{-1}	2
Pb	2	N.D.	N.D.	N.D.	N.D.	40
Sn	N.D.	N.D.	N.D.	N.D.	N.D.	4.10^2
Mg	50	50	N.D.	7.10^{-1}	5	20
habit	plates	plates	rods	plates	plates	ingots

*) Results obtained from Dr. N.W.H. Addink
‡) Results obtained from Dr. H.A. Das
**) Inhomogenous
N.D.: Not Detectable

temperature above that of the melt and results in melting of the nucleus. To allow nucleus formation therefore any latent heat must be dissipated and once the nucleus is formed, its rate of growth is determined only by the rate at which the heat of solidification can be removed from the solid-melt interface. The heat of crystallization can be taken up by the walls of the containing crucible or by a supercooled melt.

As the solidification proceeds a faster growing seed usually outstrips the others and a single crystal is eventually produced.

The arrangement adopted in our experiments is shown schematically in in fig. 3.4.

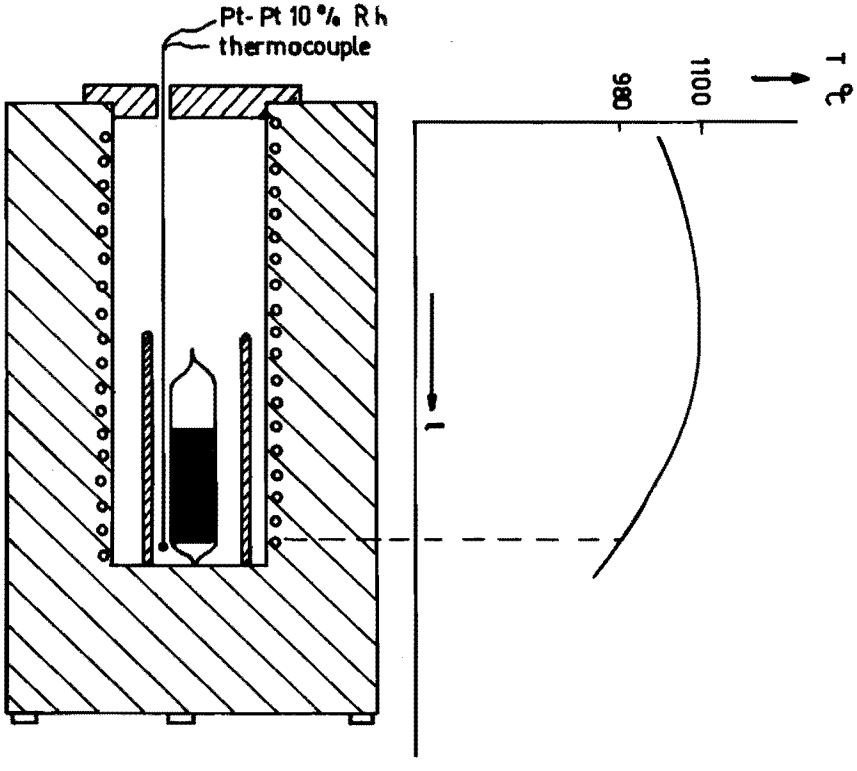

Fig. 3.4. Furnace and temperature profile during the melt-growth process.

The silica vessel contains an alumina crucible.*) Both underwent the cleaning procedure as described before and are subsequently vacuum baked. The Al_2O_3 crucible is filled with polycrystalline GaS powder, the silica vessel is evacuated (10^{-3} mm Hg),sealed off and placed in a temperature gradient in a vertical furnace.
The melt is brought to about 980°C and slowly cooled at the rate of 1° per hour to about 900°C by means of a clock work driven variac which reduces the current. Further cooling to room temperature is done in air.

From the ingots produced, monocrystalline slices can be cut, having their *c*-axes normal to the plane of the crystal plate. Plates which measure up to 800 microns in thickness with an area of 5 x 5 mm^2 can be obtained. Spectrografic analysis of this melt grown material is presented in column 7 of table 3-II.
The analysis shows a rather high impurity content in this melt grown material.
It is not quite understood why the concentration of Na, Pb and Sn, is so high, however as nothing is known about the segregation constant of the various elements in GaS, nothing definite can be said about the increase of impurities as compared to the concentrations given in table 2-I.

3.2. Crystal habit

3.2.1. Variation in habit

The platelike habit is the dominant form for gallium sulphide crystals produced by the iodine transport technique as long as the amount of iodine used exceeds a certain value.
This value lies around 0.25 mg cm^{-3} of iodine as is shown in tabel 3-I When the concentration of the halogen is decreased, thin ribbons and needles become dominant. At the same time a noticeable decrease in the growth rate is observed and the yield of useful platelets becomes low.

*) Purox 99.7°/o pure Al_2O_3 from Morganite Ltd. England.

In this way the situation becomes comparable with the one found in sublimation.

Crystals grown by sublimation show a rodlike and ribbonlike habit although variations depending on the degree of supersaturation have been noticed: rods and thin platelets are formed at growth temperatures of 900°C with the supersaturation ratio σ having a value of 1.9*). Growth temperatures lower than 900°C are favourable for the formation of thin needles and thin ribbons. The supersaturation is than correspondingly higher.

Both rods and needles form the majority of the crystals produced per batch in sublimation experiments. They have never been seen to grow directly on the tube walls, but always on plates (fig. 3.5.) or on polycrystalline deposited material.

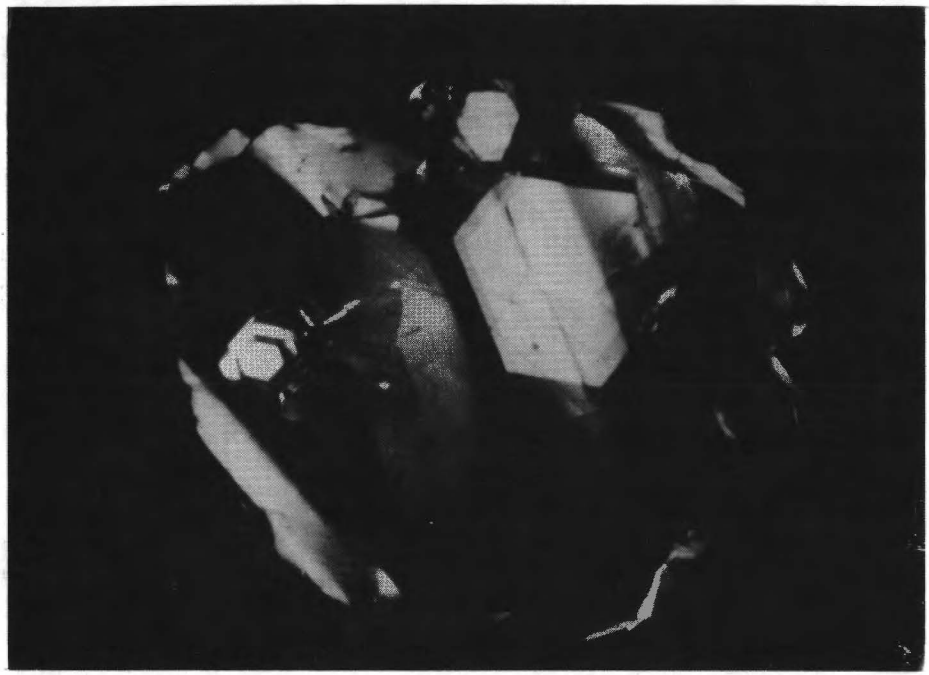

Fig. 3.5. Part of a sublimation-grown platelet; the onset of a hexagonal rod is clearly visible (60x).

*) The saturation value α is the ratio of the vapor pressures of GaS at evaporation temperature to the equilibrium pressure at the growth temperature. The supersaturation $\sigma = \alpha - 1$.

Apart form the fact that needles grow at a higher supersaturation than rods there is a difference in their habit. Both consist of layers stacked on top of each other, but needles have smooth well developed faces and pencil sharp growing ends - fig. 3.6. and 3.7. a. The faces of the rods are not so well developed, branching off at the top is sometimes observed, fig. 3.7. b and c.

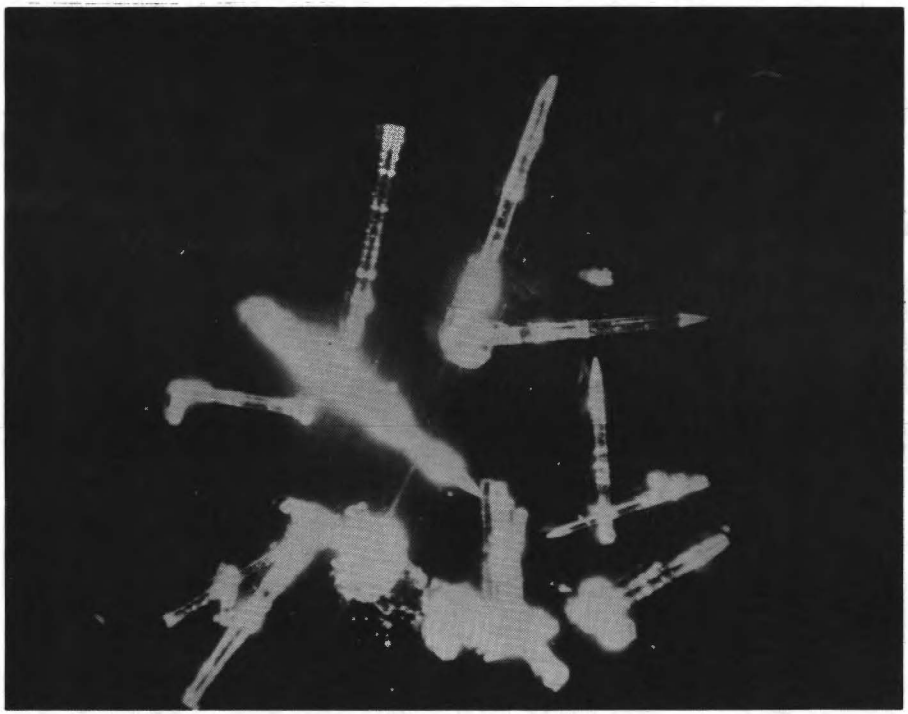

Fig. 3.6. Sublimation-grown needles; growth temperature 870° C. (10x).

Variation in growth habit has been observed by many authors. Samelson (S_{11}) noticed different crystal habits in experiments with pure ZnS; in the presence of H_2S gas, crystal growth varied from hexagonal rods to flat plates, crystals grown in vacuum had structures varying from hexagonal to cubic. In view of these differences in habit Samelson concludes that the crystal habit of ZnS is sensitive to the supersaturation ratio and in this way may be related

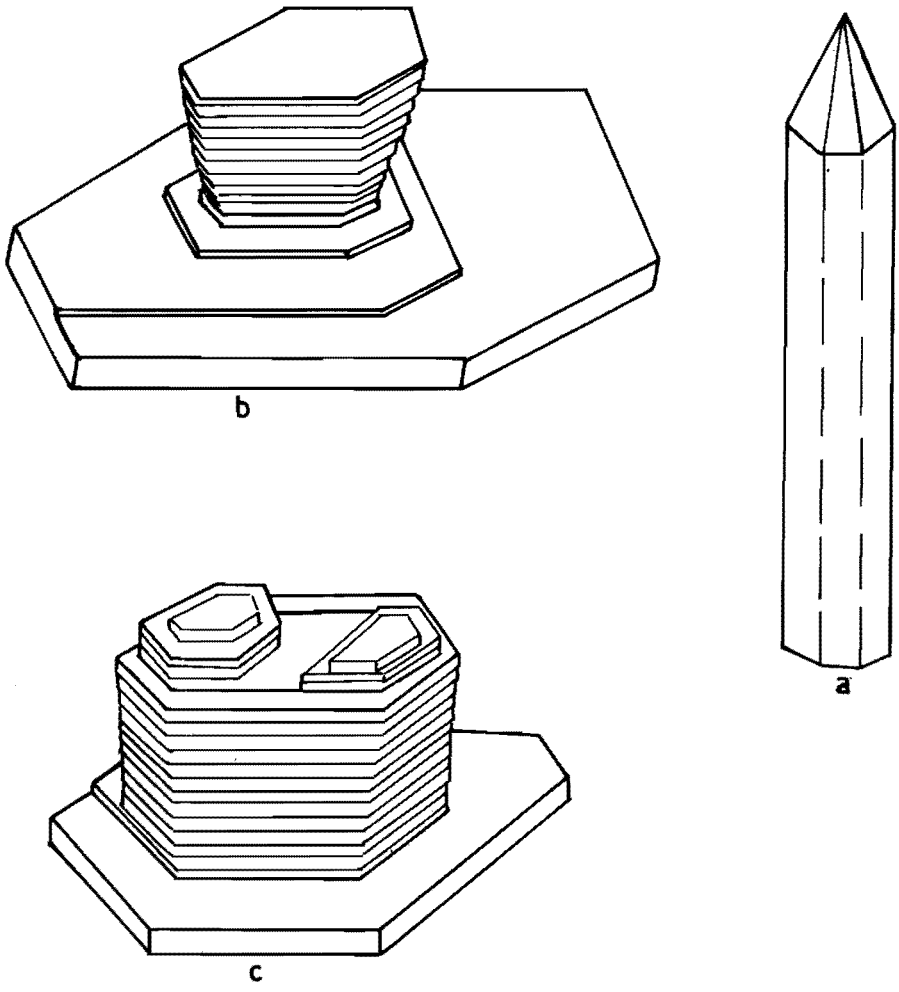

Fig. 3.7. Products of sublimation growth experiments; (a) needles with smooth faces and sharp growing ends, (b) rods with the stacking of the layers clearly visible, (c), branching off at the top is sometimes visible.

to a difference in growth mechanism. Dev and Lauer (D_1) observed a hampering effect of dopant atoms on the growth of ZnS.
The study of the growth of ice crystals described by Mason (M2) suggests that variation in crystal habit can be attributed to a surface property and that the change in habit may be induced by adsorption of traces of certain impurities.
The habit change of GaS crystals from essentially platelike to columnlike, reflects the change in relative growth rates of the basal plane and the prism faces with decreasing amounts of iodine.
It seems that the presence of the atoms of this impurity, hampers growth along the *c*-axis and favours growth perpendicular to this axis.

3.2.2. Growth mechanism

Microsopic examination of iodine grown crystals revealed hexagonal growth spirals orginating from screw dislocations fig. 3.8. No such spirals have been observed on sublimation grown crystals. The evidence so far suggests that, although spiral growth around dislocations does occur on iodine transported crystals, this is not the principal growth mechanism for GaS. It is assumed that the principal growth occurs at a high supersaturation and proceeds by two dimensional nucleation leading to the formation of hexagonal terraces.
These terraces can readily be seen with the naked eye on all platelike crystals and with a low magnification on the growth ends of rods. Eventually when the supersaturation has dropped to a lower value, spiral growth may be expexted.

3.3. Doping experiments

Polycrystalline GaS with known amounts of Cu and Zn was prepared by adding the calculated amount of foreign ions in the form of an agueous solution of the corresponding sulphate and nitrate to the powdered GaS and evaporating to dryness at 120°C.

Fig. 3.8. Growth spirals on an iodine-grown crystal, the dislocations have opposite screw direction (2000x).

The mixture is then heated at 800°C in argon gas in order to decompose the sulphate or nitrate. The resulting powder is afterwards used in an iodine transport process and in a sublimation experiment to obtain single crystals.

In attempts to dope GaS with sodium, a solution of sodium iodide was used. This was evaporated to dryness at 120°C in a quartz reaction tube. Polycrystalline GaS and iodine were then added and the tube was sealed off and used for a transport process to obtain single crystals. In the case of Cu and Zn a solution containing 10^{-4} mole of the metal per mole GaS was used, in the case of Na a solution containing $7.5.10^{-5}$ mole sodium per mole GaS was used.

Spectrografic data of single crystals are given in tabel 3-III.

TABLE 3-III

Analytical data of doped samples (weight ppm)

dope	polycrystalline bulk after heating at 800°		single crystals grown by iodine technique	single crystals obtained by sublimation technique
	calc.	found		
Cu *)	60	30*)	0.6 *)	0.3 *)
Zn *)	65	N.D. *)	N.D. *)	N.D. *)
Na †)	17	N.A.	20 †)	-

*) Spectrografic data obtained from Dr. N.W.H. Addink, Philips Res. Lab. Eindhoven

†) Neutronactivation data obtained from Dr. H.A. Das, R.C.N. Petten

N.A. = not analysed N.D. = not detectable

It can be seen that the copper concentration in the bulk is increased, compared to the concentration of Cu in boat prepared GaS (see table 2-I) but Cu is not transported and this amount is not found back in the single crystals. Zinc cannot be detected in the bulk material, it probably evaporates from the bulk during the heat treatment at 800°. The sodium concentration detected in the iodine-grown single crystals corresponds with the amount added to the polycrystalline starting material.

3.4. Conclusions

Growing single crystals with the iodine transport process is the easiest method, which produces the largest crystals in the shortest time. The sublimation technique and the melt growth technique have the advantage of producing iodine free crystals, but the yield of useful crystals is poor compared to the first method.

In comparing analytical data of crystals grown by the different techniques - table 3-II - with the data of starting materials - presented in table 2-I - the following may be remarked.

The high Al concentration present in the starting material - due to the fact that an aluminum boat was used - is not found in vapour grown crystals, the content in the melt grown sample is higher than in the vapour grown product.

The amount of Cu in vapour grown crystals is always less than in the starting material except in the case of the sublimation grown rods.

The Si concentration in crystals grown by the iodine process changes depending on the starting material.

The amount of Na in vapour grown crystals is low when the starting material contains a low concentration, the increase of it in melt grown material is surprising. The same can be said of Pb and Sn.

However as nothing is known about the segregation constants of dissolved foreign atoms in GaS, only speculations can be made about the reason for the high concentration of Na, Pb and Sn in melt grown material.

The results of the doping experiments are in good agreement with the above mentioned results as far as Cu and Na are concerned. In general one can say that the concentration of impurity atoms in the bulk material and in the crystal are of the same order of magnitude. Probable exceptions are the elements Al and Cu.

Chapter 4

MEASUREMENTS OF THE DARK CONDUCTIVITY AS A FUNCTION OF TEMPERATURE

In this chapter attention is paid to the procedures used in measuring the temperature dependence of the dark conductivity of *n*- and *p*-type crystals.

Measurements of the dark conductivity of *n*- and *p*-type crystals are carried out in the temperature range 90°-450°C. Preliminary experiments up to 250° were performed with a sample holder of teflon. For measurements at higher temperatures we designed a quartz sample holder.

Liquid gallium - which had shown itself preferable to alloyed indium - was choosen as contact material. From the measurements of the conductivity versus reciprocal temperature, activation energies can be calculated, which give an idea about donor and acceptor depth.

All the measurements were carried out in an argon atmosphere to prevent oxydation of the crystals and the metallic electrodes.

4.1. The procedure of Van der Pauw

Measurements of the conductivity were performed with separate current and voltage probes in order to eliminate contributions due to contact resistances.

The method most appropriate for measurements on plane parallel crystals of arbitrary shape is that described by Van der Pauw (P_2).

For the evaluation of the specific resistivity of such a flat sample, four electrodes are placed in an arbitrary way along the periphery of the sample (see fig. 4.1) and two resistance measurements are then carried out.

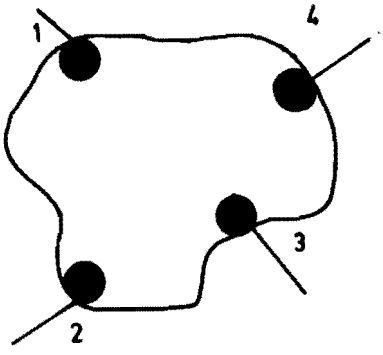

Fig. 4.1. Four electrodes placed around the periphery of an arbitrarily shaped plan-parallel GaS crystal.

When a current I_1 is passed through the contacts 1 and 2 a voltage V_1 appears across the contacts 3 and 4. The ratio V_1/I_1 is represented by a resistance R_1. In an analogous way a resistance R_2 is determined by passing a current I_2 through the electrodes 2 and 3 while the voltage V_2 is measured across 1 and 4.

The specific resistivity ρ can then be calculated by using the equation:

$$\rho = (\pi d/2\ln 2).(R_1 + R_2).\, f\,(R_1/R_2) \qquad (4.1)$$

in which d is the thickness of the sample. The function $f\,(R_1/R_2)$ is presented in graphical form by Van der Pauw in his article (P_2).

According to the theory, the following conditions have to be fulfilled.

1. The contacts must be at the circumference of the sample.
2. The contacts must be sufficiently small.
3. The sample must be homogeneous in thickness.
4. There must be no isolated holes in the sample.

The author emphasizes the point that if conditions 1 and 2 are not fulfilled, an error is introduced in the evaluation of the resistivity. However the influence of the contacts on the measurements in general can be diminished by giving the crystal the shape of a four-leave clover. This is done by making incisions in the sample, see fig. 4.2.

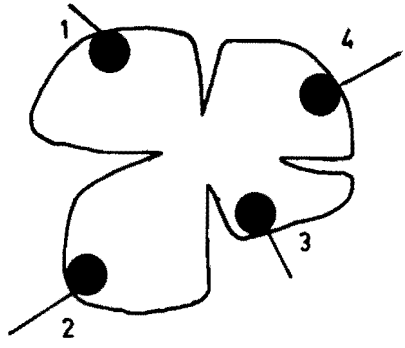

Fig. 4.2. GaS crystal with the four incisions between the electrodes.

In order to determine experimentally the aforementioned contact influence, the conductivity of a crystal furnished with liquid gallium contacts, was measured between 50°-250°C before and after incisions were made. The conductivity versus reciprocal temperature of this sample is presented in fig. 4.3.

It can be seen that in this case clover-shaping the sample does not affect the conductivity very much which means that the influence of the contacts can be neglected.

Another possible influence on the conductivity can be expected to come from inhomogeneities in the crystal. This effect can also be detected by clover-chaping the crystal; measurements performed with and without incisions made on it will show a different average specific conductivity at a constant temperature, because in clover-shaping, parts of the crystal are removed.

Furthermore a variation of the ratio R_1/R_2 with temperature can also be caused by inhomogeneities. This was investigated by Van Daal (D2) in his work on silicon carbide. Such is the case when the activation energy is a function of the impurity concentration. When the temperature is changed the different regions of the crystal will show a different temperature dependence. Due to this fact R_1 and R_2 will exhibite a different temperature dependence.

On account of the above mentioned facts the variation of the ratio R_1/R_2 has been included in fig. 4.3 for crystal S_8 before and after incisions were made on it.

Whether condition number 4 is fulfilled is easily determined; even small holes, if any, are revealed by microscopic examination of the

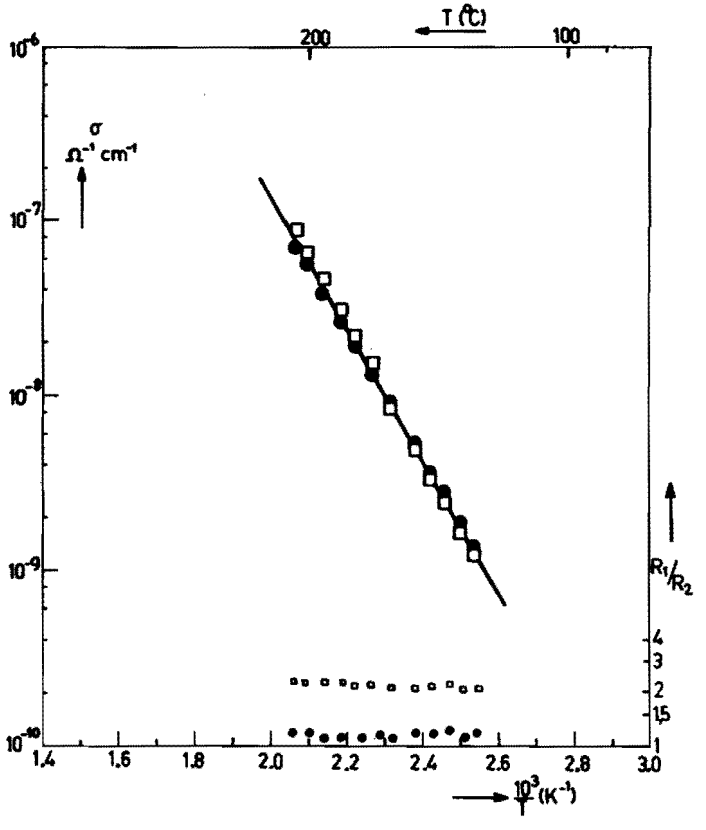

Fig. 4.3. The specific dark conductivity versus $10^3/T$ of crystal S_8. The measurements were performed without incisions made on the sample, (●) and with incisions, (□). R_1/R_2 values are also presented.

sample surface, a procedure which is performed before the crystal is mounted on the sample holder.

The majority of the crystals used in our work were between 10 and 20 microns thick. A variation in thickness of 20°/o was accepted. This amounts to a variation of 4 microns at the most.

The crystal thickness is measured mechanically with a Mikrokator SY. 510-4 with and adjustabel measuring range and adjustable measuring force.

4.2. Electrical contacts and sample holder

4.2.1. Contact materials

The choice of the contact material proved to be rather difficult and a wide variety of metals and alloys have been tried, and are still used by investigators in our group (K_2, H_6, V_1) as well as in other laboratories (M_3). Only a limited number has proved to meet the requirements of being able to withstand repeated temperature variations while non rectifying at the same time. Hg-In and In-Ga mixtures were used in the earliest measurements by Kipperman and Van der Leeden (K_2, L_4) in their work on photoconductivity and photo-Hall effect. Both mixtures can be pasted onto the crystal which thereafter is heat treated. At 350°-400°C in a hydrogen atmosphere the Hg-In looses its mercury, thereby forming indium contacts.

Indium contacts, produced either in this way or by direct alloying with the metal, have been used in preliminary conductivity versus temperature measurements up to 200°C. However under prolonged heating at 250°C and higher, or during repeated temperature variations, the contact material reacts with the bulk of the crystal and eventually the area around the electrodes is disconnected from the crystal.

Other low melting metals like Sn, Pb or Zn did not meet the requirements for one or other reason.

More promising are vacuum evaporated gold contacts, or evaporated indium contacts which are gold coated after being heat treated, (V_1), and liquid gallium contacts. In the majority of our measurements, liquid gallium was used for the electrodes.

4.2.2. Sample holder

In the earliest experiments a teflon holder was used but the majority of our measurements was carried out between 50°-400°C with a quartz sample holder.

Quartz has proved to be useful up to high temperatures. The insulation resistance of the holder was determined between 100° and 500°C. It varied from $2.10^{12}\ \Omega$ at 100°C to about $10^{12}\ \Omega$ at about 450°C. Compared with a high-resistance sample like S_8 the sample holder was approximately 10^6 times better at about 400°C.

The holder was made of quartz*) tube with one end in the form of a spoon (see fig. 4.4a). The other end has a ground glass-joint head, to which a metal jacket is fastened.

An inner container of quartz and an outer container of stainless steel complete the apparatus; the quartz container can be fitted to the glass-joint head, enabling measurements in any desired atmosphere while the metal container can be fitted to the metal jacket, enabling measurements in complete darkness. On the spoon-shaped end, a quartz cup (see fig. 4.4c and d) is fastened. The crystal is placed in this cup on four small gallium bearing platforms. Platinum-Rhodium**) wires are drawn through capillaries in the bottom of the cup. By flattening them out the small platforms are obtained, which support the small gallium pellets used as electrodes.

The distance between the gallium contacts is of the order of 5 mm, the diameter of a liquid contact is about 1 mm.

A sample is placed on the four pellets and a quartz cover (see fig. 4.4c) fitting snugly the inside of the cup, is placed on top of the crystal, pressing it onto the gallium electrodes and at the same time minimizing movements of the crystal relative to the liquid contacts.

Coupled to the Pt-Rh wires are Pt measuring-leads which are drawn through four capillaries in the holder and soldered to four connectors in the metal jacket, (see fig. 4.4b). The metal jacket also contains two more connectors for thermocouple wires***) and an inlet and outlet tube for the argon. A ceramic switch, which enables rapid changing from one current voltage combination to the next, can be coupled to the four connectors in the metal jacket.

---

*) PURSIL 453 type from Quartz et Silice, France

**) Pt-10°/o Rh wires are used, as Pt is not satisfactory probably due to poor wetting by the liquid gallium.

***) Iron-Constantaan is used for the thermocouples

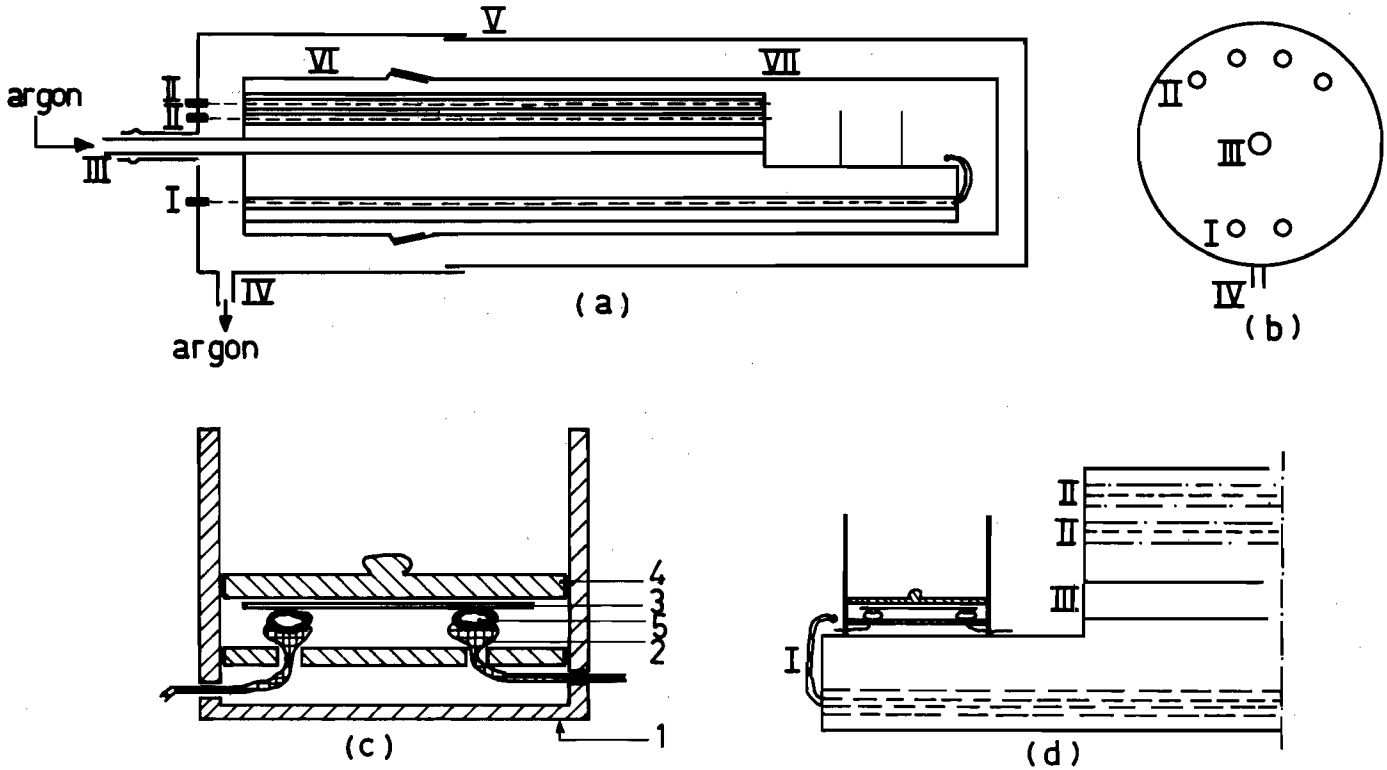

Fig. 4.4. Longitudinal section through the quartz sample holder (a, d), front-side view of the metal head (b) and side view of the cup (c). Components are: (I) connectors receiving thermo-couple wires, (II) connectors receiving Pt-measuring leads, (III) gas supply inlet, (IV) gas outlet, (V) metallic container, (VI) quartz head with ground glass-joint, (VII) quartz container.
(1) quartz cup, (2) Pt-wires bearing gallium droplets, (3) crystal, (4) quartz cover fitting inside the cup, (5) gallium droplets.

The tube system is situated in a horizontal electrically heated furnace as shown in fig. 4.5

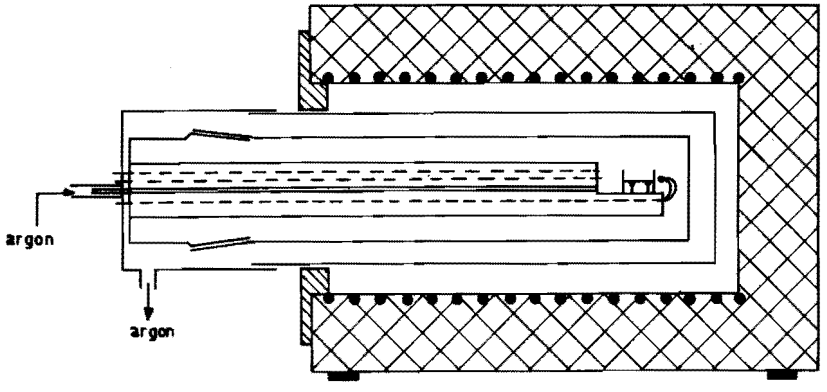

Fig. 4.5. Electrical furnace used in the conductivity measurements.

The temperature of the crystal is registered on a recorder, and variations in crystal temperature can be achieved by changing the current through the furnace manually. Prior to each measurement, the whole tube system is swept clean of oxygen by passing a flow of purified and dried argon through it; during the measurements a reduced stream is passed over the crystal to prevent oxydation of crystal and electrodes.

4.3. The measuring circuit

For measurements of samples with resistances up to $10^{12}\ \Omega$,the d.c. circuit shown in fig. 4.6 is used. The conditions required for these measurements are the following:

1. Independent measurements of current and voltage.
2. The use of voltmeters with a high input resistance.
3. Shielding of the high resistivity part for stray signals.
4. The use of low capacity leads from sample to current-and volt-meters.
5. A sample holder with an insulation resistance better than $10^{12}\ \Omega$ at room temperature.

This circuit is a modified form of the one described by Fischer et.al. (F_2)*)

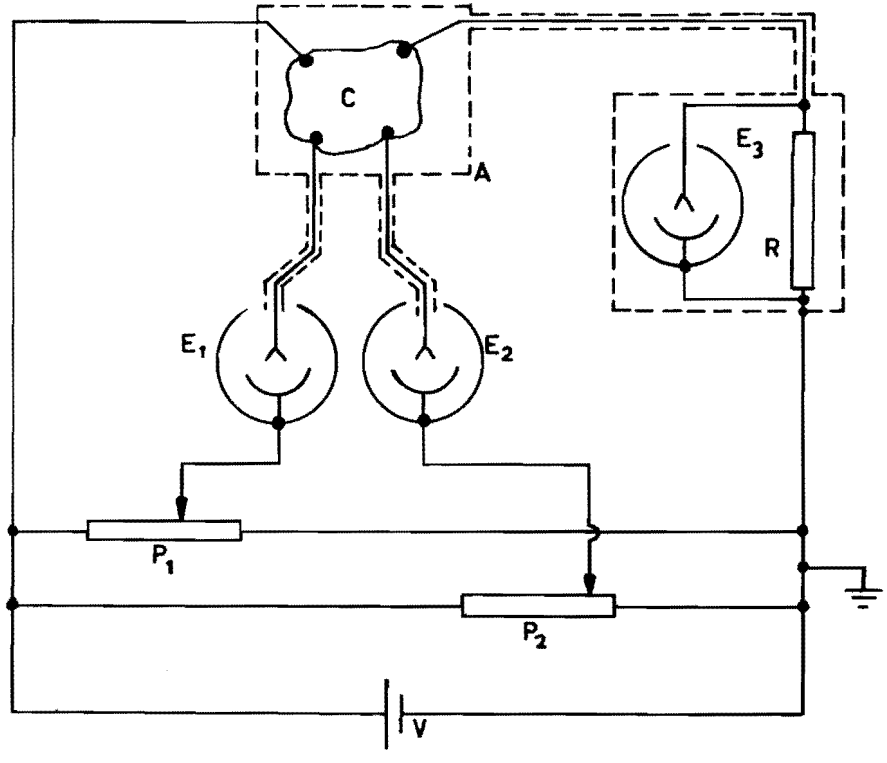

Fig. 4.6. The measuring circuit; (A) = shielding of the high resistivity part, (C) = the crystal; (E_1 and E_2) = zero detectors (Keithley 200B), (E_3) = Ampere meter (Keithley 610B) (P_1, P_2) = potentiometers; (V) = stabilized voltage supply (Delta).

In all measurements 100 volts was applied and the low dark current is detected with electrometer E_3. Electrometers are used for voltage measurements because of the high resistances of the samples. They are used as null indicators and are balanced with the aid of two grounded potentiometers P_1 and P_2.

*) The idea of the modification is due to mr. Kipperman of our laboratory.

Electrometer E_1 is brought to zero by means of P_1, and P_2 is used to compensate the voltage on the E_2 side, which thus permits a direct reading of the voltage drop across the potential leads. The input resistance of the meters E_1 and E_2 is about 10^{14} Ω, the insulating resistance of the sample holder is better than 10^{12} Ω and the switch resistance is 10^{14} Ω.

With a voltage of 100 volts applied across the current contacts, a leakage current of 10^{-12} Amp. arises, which means that currents down to 10^{-11} Amp., i.e. about ten times the leakage current, can be measured with reliability.

Shielding of the potentiometer circuits is avoided on account of their grounded circuits, but that of the high resistance part is necessary. The voltage leads from the crystal to E_1 and E_2 and the current lead to E_3 are coaxial cables of minimum length, to minimize the response time. With an input capacitance of about 10 pF for the electrometers and a cable capacitance of about 1 pF per cm, this amounts to about 30 pF for meters and cables (of 20 cm length) in the above described circuit. For the earliest measurements with *impure* crystals having resistances in the order of 10^{11}-10^{12} Ω, this means a response time of 3 to 30 sec. at room temperature, which amounts to a wait of about 15-150 sec. For the *purer* *n*-type crystals having a resistance of about 10^8 Ω or less, this time lies in the order of 2.10^{-2} sec or less.

At room temperature the two most favourable current-voltage combinations are determined.

When the sample holder is cleaned of oxygen by a stream of argon, the furnace is heated up and both current and voltage are measured. This is done every four degrees, while the crystal temperature rises slowly and continuously.

4.4. Accuracy of the measurements

As to the accuracy achieved in the determination of the conductivity the following remarks can be made.

Potential differences were measured by compensation using two electrometers as null indicators, while a third one was used to measure the current. For the conductivity σ the random relative error can be estimated to be 6°/o, which becomes $\approx$ 0.03 times the unit of the log scale.

The deviation in temperature reading amounts to about 3 degrees, which is $\approx$ 0.01 times the unit of the temperature scale at a temperature of 500 K.

Other factors which may effect the measurements are the size of the contacts and the crystal thickness. Errors introduced by these factors can be considered to be systematic.

An estimation of the order of magnitude of the error introduced if the contacts are of finite size and on a distance from the circumference is given by Van der Pauw (P_2). This amounts to a maximum systematic error of 2°/o.

As already discussed in section 4.1. the majority of our crystals are non uniform in thickness; a variation in thickness of 20°/o was accepted.

The ratio R_1/R_2 is not constant during the measurements, the variation in this ratio - between 50° and 400°C - differs from crystal to crystal. For the various crystals the variation from an average R_1/R_2 value lies between 5 and 12°/o*).

One reason for such a variation is the change in geometry of the liquid gallium contacts during the heating of the crystal. Another possible reason is sample inhomogeneity - as has been discussed in section 4.1 - which can be caused by diffusion of impurities at elevated temperatures during the performance of the measurements.

*) An average value of the ratio is presented for every sample in the discussion of the measurements. (tables 4-I and 4-IV).

4.5. Results of the conductivity measurements as a function of temperature

4.5.1. Results for n-type crystals

In fig. 4.7 the dark specific conductivity σ versus reciprocal temperature is presented for two groups of *n*-type crystals.
The first group includes the samples S_4, S_7, S_8, and S_{16}, the second group the samples S_{13}, S_{21}, S_{25}, S_{27}, S_{43}, and S_{51}.
Crystals from group I originated from polycrystalline material synthesized without an alumina boat; for all other *n*-type crystals the starting material was prepared in a boat.
Most of the crystals are from different batches and they are all produced by the iodine process with an iodine concentration of 4 mg/cm^3,
In table 4-I the activation energy ε of the conductivity σ is given for the ten crystals, together with the average value of the ratio R_1/R_2 see section 4.4

TABLE 4-I

activation energy ε of the conductivity, and average value of R_1/R_2

	S_4	S_7	S_8	S_{16}	S_{13}	S_{21}	S_{25}	S_{27}	S_{43}	S_{51}
ε (eV)	0.81	0.78	0.76	0.80	0.41	0.60	0.40	0.48	0.48	0.60
average R_1/R_2	3.0	2.7	2.2	2.5	2.2	1.5	1.5	1.3	1.5	1.2
group	I				II					

The Hall mobility u_H was determined by Kipperman and Vermeij (K_8, V_1). They found for *n*-type GaS a temperature dependency of the form

$$u_{Hn} = 16.(T/300)^{-2.4}\ \text{cm}^2/\text{Vs} \qquad (4.2)$$

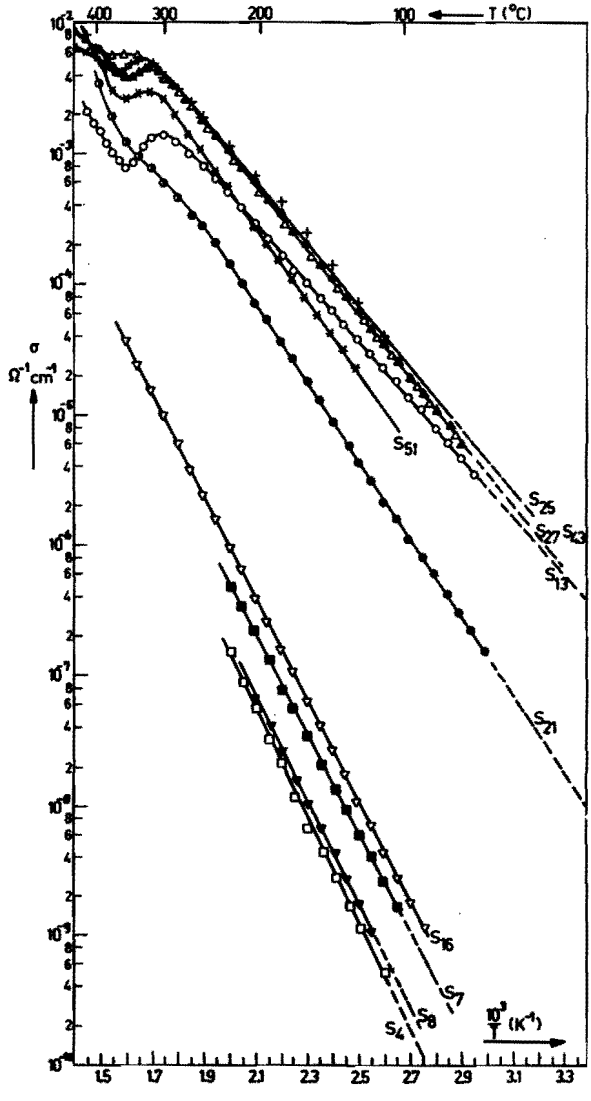

Fig. 4.7. Conductivity (σ) versus $10^3/T$ of two groups of n-type crystals. (●) : S_{21} warmed to 250°C and kept there for 24 hours; (●) S_{21} warmed from 250–400°C.

Using this mobility, the free electron concentration as a function of temperature can be calculated for the two groups of crystals. The result is presented in fig. 4.8. An analysis of these diagrams reveals the following.

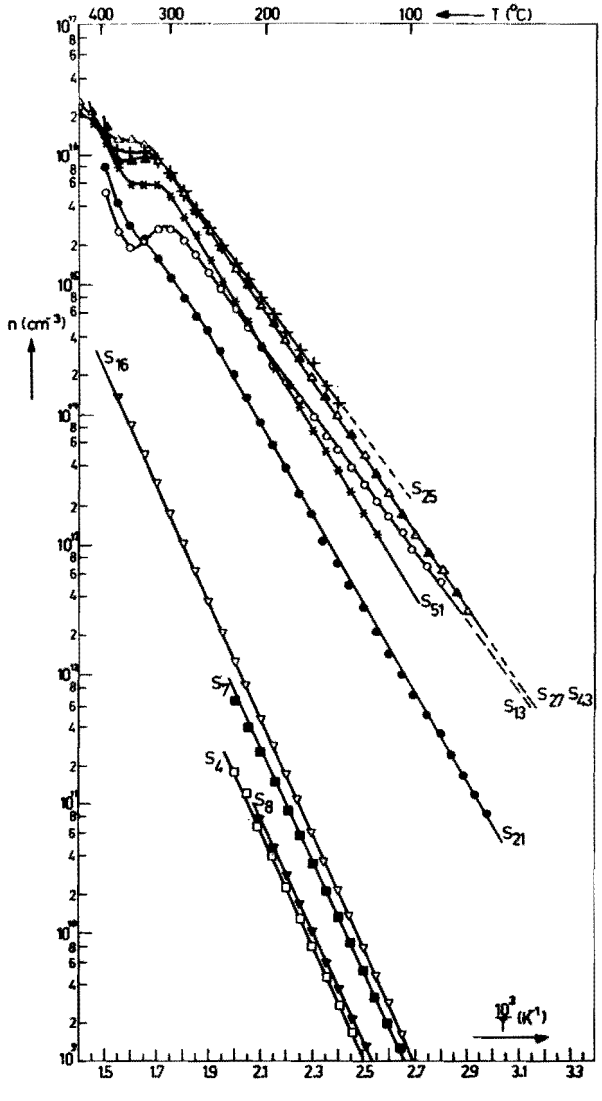

Fig. 4.8. Concentration of free electrons (n) versus $10^3/T$ of two groups of n-type crystals.

From the slopes of group I crystals, activation energies of $n = f(10^3/T)$ lying between 0.82 and 0.85 eV can be calculated. There is no indication that the electron concentrations tend towards an exhausted range. The group II crystals have slopes from which energies lying between 0.50 and 0.66 eV can be calculated. Here the electron concentrations of the various samples show a tendency towards a constant value at temperatures around 300-350°C.

4.5.2. Heat treatment effects

The influence of a heat treatment on the dark conductivity of *n*-type crystals was investigated. Each sample used in these experiments was sealed under vacuum in a small ampoule, heated to approximately 450°C and kept at this temperature for about one hour*).
It was then either quenched to room temperature - by immersing the ampoules in water - or very slowly cooled to room temperature (in 11 hours) in the furnace, and thereafter mounted on the sample holder. To exclude light, the ampoules were wrapped in aluminium foil. The conductivity of the crystals was measured in heating and cooling cycles. In fig. 4.9, 4.10 and 4.11 the concentration versus $10^3/T$ is shown for these three crystals. For S_{41} the measurements were performed in the following sequence:

S_{41}-1: Before carrying out the heat treatment, the conductivity was measured while the crystal was warmed to 250°C and subsequently while it was cooled. Thereafter the crystal underwent the heat treatment at 450°C which was followed by *very slow cooling* to room temperature.

---

*) On account of practical difficulties, the heat treatments could not be carried out in the setup used for the conductivity measurements.

S_{41}-2: The conductivity was then measured while the crystal was warmed to 400°C and also during the subsequent cooling.

S_{41}-3: Again the conductivity was measured while the sample was continuously warmed to 250°C and thereafter cooled. For S_{41} the average R_1/R_2 was 1.4.

For S_{44} the sequence was:

S_{44}-1: Before carrying out the heat treatment, the conductivity was measured while the crystal was warmed to about 400°C and subsequently while it was cooled.

Thereafter the heat treatment at 450°C was given, followed by *rapid cooling* to room temperature.

S_{44}-2: The conductivity was then again measured while the crystal was warmed to 400°C and cooled.

S_{44}-3: The conductivity was measured again while the crystal was warmed up, this time the experiment had to be stopped at about 320°C on account of contact troubles*). The average ratio R_1/R_2 was 1.0 for S_{44}.

The conductivity of S_{45} was not measured before the heat treatment was given. After having been heated at 450°C for one hour the crystal was *very slowly cooled* to room temperature.

The conductivity was then measured while the crystal was warmed to 400°C. The average ratio R_1/R_2 was 1.3. for this sample. The three samples, S_{41}, S_{44}, and S_{45} were grown with an iodine concentration of 4 mg/cm^3.

From these results it can be deduced that there is a difference in the temperature dependence of the electron concentration and thus of the conductivity, between the crystals which are cooled slowly - like S_{41}-2 and S_{45} - and the crystal which is rapidly cooled, like S_{44}-2. This effect has disappeared when the slowly cooled samples have been warmed again to a temperature of about 400°C and subsequently cooled during the conductivity measurement.

---

*) This is not surprising, the measurements of one cycle with a maximum temperature of 400°C takes about eight hours and a complete experiment like in the case of S_{41} or S_{44} takes about a week.

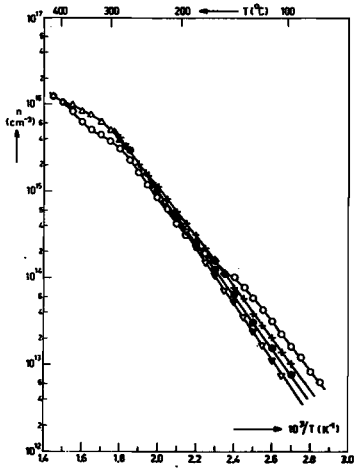

4.9

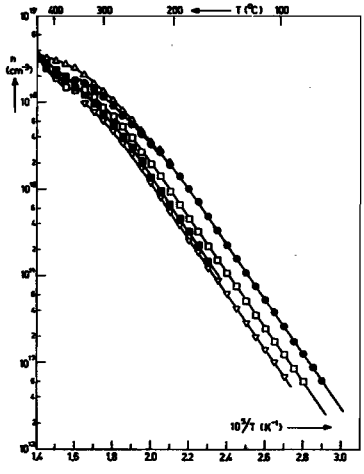

4.10

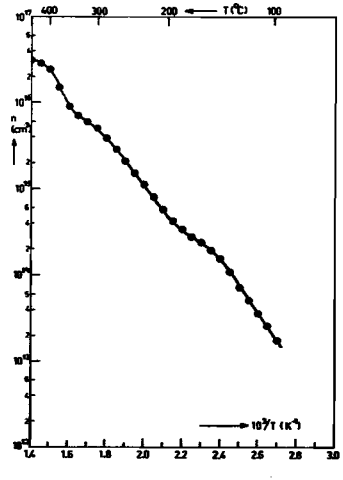

4.11

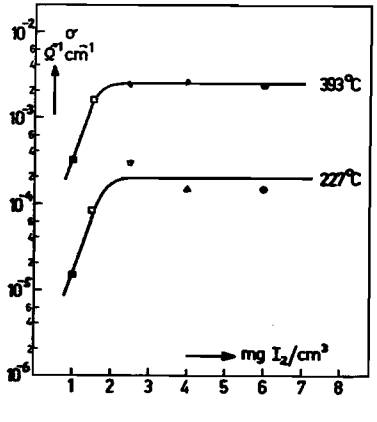

4.12

Fig. 4.9. Concentration (n) versus $10^3/T$ of the n-type crystal S_{41}; (S_{41}-1) heating (+) and cooling (●) cycle; (S_{41}-2) heating (o) and cooling (Δ) cycle; (S_{41}-3) heating (▼) and cooling (▽) cycle.

Fig. 4.10. Concentration (n) versus $10^3/T$ of the n-type crystal S_{44}; (S_{44}-1) heating (●) and cooling (Δ) cycle (S_{44}-2) heating (□) and cooling (■) cycle; (S_{44}-3) heating (▽).

Fig. 4.11. Concentration (n) versus $10^3/T$ of the n-type crystal S_{45}; (●) heating measurement.

Fig. 4.12. Conductivity (σ) as a function of iodine concentration used in the growth ampoule.

For this reason such effects are not observed in other *n*-type crystals like those mentioned in 4.5.1. for example - because the history of those crystals is different. The silica tubes in which the crystals are grown, are taken out of the furnace and first cooled at one end to collect the gallium iodide vapours (see section 3.1.1) and thereafter completely immersed in water. The time needed for complete cooling in such a procedure is much shorter than the eleven hours needed for S_{41}-2 and S_{45} to cool to room-temperature.
No attempts will be made to present a calculation based on semiconductor statistics for the small dips in the curves; they themselves are not regions of exhaustion since their bends are much to sharp. The effects observed are probably due to atomic interactions like a dissociation of associates or clusters. It must be noted that S_{41}, S_{44} and S_{45} in fact also belong to the group which we have denoted as II. Their concentrations tend also towards an exhausted region at $\approx 10^{16}/cm^3$. Further attention will be given to them in section 4.6 and 4.8.

4.5.3. Influence of the iodine concentration on the conductivity

To determine the influence of the amount of iodine - used in the growth process - on the conductivity, crystals produced wich iodine concentrations ranging from 1 to 6 mg/cm^3 were investigated.
From the two isotherms shown in fig. 4.12 - one at 393°C and one at 227°C - it can be concluded that the conductivity becomes independent of the amount of iodine when the concentrations exceeds a value of 2.5 mg/cm^3.

4.6. Interpretation on the basis of semiconductor statistics.

When we assume a bandscheme with a single donor, application of semiconductor statistics leads to the following relation between the concentration and the ionisation energy of the donor:

$$\frac{n^2}{(N_D - n) \cdot N_C} = e^{-E_D/kT} \quad , \qquad (4.3)$$

where n = concentration of electrons (cm^{-3})
N_D = concentration of donors (cm^{-3})
N_C = density of states in the conduction band (cm^{-3})
E_D = ionisation energy (eV) of the relevant donor, that is the difference in electronic energy between the bottom of the conduction band and the donor level*) **).

It is seen that apart from the temperature dependence of N_C, for a low degree of ionisation ($n < N_D$), n is proportional to $e^{-E_D/2kT}$. For the group I crystals this leads to values of E_D varying between 1.6 and 1.7 eV. These values for the ionisation energy are invalid for two reasons.

1. In this model no acceptor is included and this is inconsistent with the degree of purity of our crystals.
2. Such a deep donor is not very probable.

For a model which takes compensation into account, the relation between the various concentrations and the donor ionisation energy can be written as

---

*) It should be noticed that in formula 4.3 and in all further considerations regarding the statistics, the absolute values of the donor, the acceptor and the Fermi energies (i.e. $E_C - E_D$, $E_A - E_V$, $E_C - E_F$ (or $E_F - E_V$)) are used and are denoted by E_D, E_A and E_F respectively.

**) Here the degeneracy factor g of the level, is not taken into consideration; in fact the E_D represents an effective level $E_{D\ eff.}$ which is related to the real value E_D by the expression:

$$E_{D\ eff.} = E_D - kT \ln g \text{ (see Putley, } (P_3)\text{).}$$ For g = 2, this relation becomes:

$$E_{D\ eff.} = E_D - 0.7\ kT = E_D - 0.035 \text{ eV at 600 K.}$$

In our case with ionisation energies of $\sim$ 0.6 eV and $\sim$ 0,8 eV, the differences are not of importance.

$$\frac{n(N_A + n)}{(N_D - N_A - n).N_C} = e^{-E_D/kT}, \qquad (4.4)$$

where N_A = concentration of the compensating acceptors (cm^{-3}).

With $n < N_A$ and $n < N_D - N_A$ this leads to

$$n = \frac{(N_D - N_A).N_C}{N_A} . e^{-E_D/kT}, \qquad (4.5)$$

which shows n to be proportional to $e^{-E_D/kT}$. For the group I crystals this leads to values of E_D between 0.82 - 0.85 eV.

Substituting γ_n for N_D/N_A we arrive at

$$\gamma_n - 1 = (n/N_C).e^{E_D/kT}. \qquad (4.6)$$

The ratio γ_n can now be calculated for the various crystals by using the value of E_D obtained from the slopes of the curves and substituting a value of n and the corresponding temperature in equation (4.5). For N_C the value of $10^{21}/cm^3$ - as found by Kipperman and Sliepenbeek. (K_9, S_8) - is used.

In group II the crystals give a rough indication that their free electron concentrations tend towards an exhausted range. It must be noted that we neglect the small dips or horizontal parts in the curves, on account of the fact that it is improbable that they themselves represent regions of exhaustion. As mentioned before, the crystals S_{41}, S_{44} and S_{45} belong to this group II. For this group and in particular for S_{41}, S_{43}, S_{44}, S_{45} and S_{51} values for N_D-N_A can be estimated from the slope of their curves. In addition to the value of E_D and γ_n it is now possible to evaluate N_D and N_A for these crystals.

In table 4-II the data obtained from analyses of the temperature dependence of the free electron concentration are listed. For group I the values of E_D and γ_n are presented, for group II the values of E_D and γ_n and in addition for S_{41}, S_{43}, S_{44}, S_{45} and S_{51} the values of N_D, N_A and N_D-N_A.

TABLE 4-II

Ionisation energy of donors E_D, the ratio γ_n, the concentration of donors N_D, of acceptors N_A, the concentration of sodium [Na] and N_D-N_A for group I and II crystals

crystal	S_4	S_7	S_8	S_{16}	S_{13}	S_{21}	S_{25}	S_{27}	S_{41}	S_{43}	S_{44}	S_{45}	S_{51}
figure	4.8	4.8	4.8	4.8	4.8	4.8	4.8	4.8	4.9	4.8	4.10	4.11	4.8
E_D (eV)	0.85	0.82	0.83	0.85	0.52	0.66	0.50	0.57	0.57	0.57	0.57	-	0.63
γ_n	1.08	1.5	1.05	1.95	1.18	2.45	1.24	2.03	1.80	2.03	4.16	1.80	3.54
N_D-N_A (cm^{-3})	-	-	-	-	-	-	-	-	2.10^{16}	4.10^{16}	5.10^{16}	5.10^{16}	5.10^{16}
N_D (cm^{-3})	-	-	-	-	-	-	-	-	5.10^{16}	8.10^{16}	6.10^{16}	10^{17}	7.10^{16}
N_A (cm^{-3})	-	-	-	-	-	-	-	-	3.10^{16}	4.10^{16}	2.10^{16}	6.10^{16}	2.10^{16}
[Na] (cm^{-3})	$3.5.10^{19}$ +)	$3.5.10^{19}$ +)	$3.5.10^{19}$ +)	$3.5.10^{19}$ +)	$1.8.10^{18}$ *)	$1.8.10^{18}$ *)	-	-	-	-	-	-	-
group	I				II								

+) : spectrochemical analyses from Dr. N.W.H. Addink
*) : neutronactivation analyses from Dr. H.A. Das

Furthermore the sodium concentrations [Na] as found by analyses are given in the last column. The spectrochemical data are valid for all samples of group I, the result from the neutron activation analysis is valid for S_{13} and S_{21}.
Some facts call for attention; firstly there are two different donor ionisation energies, secondly the values of the ratio γ_n indicate a high degree of compensation for samples S_4 and S_8. Thirdly analytical data for S_{13} and S_{21} show a sodium concentration which is higher than the values obtained when N_A is calculated as in the case of S_{41}, S_{43}, S_{44}, S_{45} and S_{51}.

Considering the impurities present in GaS as obtained from analyses, we regard substitutional sodium and gallium vacancies as acceptors. For the II-VI compounds ZnS, ZnSe and CdS, Dieleman et al (D_3) showed unequivocally that the alkali metals Li and Na function as acceptors.
In our case copper may also act like an acceptor, but is not taken to be prominent on account of its concentration as compared to that of Na.

Substitutional iodine as a group VII element is believed to act like a donor in our crystals. This is in accordance with the role played by substitutional iodine, chlorine and bromine in III-V and II-VI compounds. Furthermore native defects like sulphur vacancies may function as donors. Other possible donors are impurities like Si, Fe and Al but it is not probable that they are prominent. This is on account of the following reasoning:
Comparing the Si-content in iodine grown single crystals with that in sublimation grown samples - both originating from the same polycrystalline starting material - it can be seen that the concentration of this impurity remains equal in both types of crystals. The conductivity however is different, since the iodine-transported material is *n*-type, while the sublimation grown material has *p*-type conductivity. (see table 3-II)
The same reaoning can be applied to the contents of Fe and Al by comparing single crystals which have starting material prepared without a boat.

4.7. Defect-chemical considerations

In crystalline compounds at temperatures above absolute zero, atomic disorder occurs in the form of small concentrations of vacant lattice sites and/or interstitial atoms.
Of the different types of disorder possible in solids, the most important are the Schottky disorder, Frenkel disorder and antistructure disorder*).
We assume a Schottky defect situation in gallium sulphide, which means gallium vacancies and sulphur vacancies**) in equal concentrations. Exclusion of the Frenkel disorder on one of the sub-lattices is based on structure considerations; this type of disorder can be expected if one of the composing atoms in a binary compound is small and the other large. The radii of the composing elements in GaS are not differing much and sulphur or gallium in interstitial positions seems therefore unlikely.
For antistructure disorder to exist in a crystal the difference in electronegativity between the components should not be to large.

Fortunately the qualitative properties of a defect such as a sulphur vacancy in GaS is independent of the type of bonding in the component. Although GaS is neither purely covalent nor purely ionic we will consider both types briefly.

In case the compound is ionic, the removal of a neutral S atom from the lattice to the gasphase, to form S_2 molecules, will leave behind two electrons which can be considered as being trapped in the vicinity of the vacancy. They can be removed one at a time into the conduction band of the solid by thermal ionisation.
In an anlogous way the removal of a neutral Ga atom creates a vacancy, with two positive charges trapped near this defect.

---

*) A detailed description of these 3 forms and their combinations, is given by Kröger in his book: Chemistry of the imperfect crystal (K_5).

**) It must be admitted that an exact determination as to the type of defects present in a specific solid requires self-diffusion experiments.

Considering the compound to be covalent, GaS is made of Ga^{-1} $(...4s^2 4p^2)$ - whereby gallium obtains a tetrahedral sp^3 coordination - and S^{+1} $(...3s^2 3p^3)$, so that sulpher gets a trigonal pyramidal p^3 coordination with a saturated s^2 subshell.

In removing a neutral S-atom $(...3s^2 3p^4)$ to the gas-phase, six of the nine electrons available are withdrawn. Of the three electrons left, one is used by the gallium in the bonding with the other gallium (B_7), the two other electrons are as before left behind, trapped near the vacancy.

The nomenclature which will be used is the one proposed by Kröger (K_6). It is the atomic notation which has the advantage of being independent of any hypothesis regarding the bonding character of the base lattice.

A missing atom is indicated by the symbol V_S^* or V_{Ga}^*, where the asterisk is used to emphasize the fact that the removement of the atom is performed without changing the charge of the site. †)

As discussed above, the two electrons attached to the vacancy, in the case of sulphur, can be removed. This is expressed by ordinary chemical equations:

$$V_S^* \rightleftharpoons V_S^{\cdot} + e' - \text{energy}, \tag{4.7}$$

and

$$V_S^{\cdot} \rightleftharpoons V_S^{\cdot\cdot} + e' - \text{energy}, \tag{4.8}$$

where e' symbolizes an electron.

Thus a sulphur vacancy may behave as a doubly ionizable donor. In an analogous way it can be shown that the metal vacancy can function as a double acceptor ‡),

$$V_{Ga}^* \rightleftharpoons V_{Ga}' + h^{\cdot} - \text{energy} \tag{4.9}$$

and

$$V_{Ga}' \rightleftharpoons V_{Ga}'' + h^{\cdot} - \text{energy} \tag{4.10}$$

where $h^{\cdot}$ symbolizes a hole.

---

†) Which is the same as effective neutrality, relative to the lattice.

‡) In the earlier notation used by Bloem (B_8) and Kröger et al (K_7), ions were removed: an anion (S^{2-}) vacancy was presented by $V_S 2-$, the empty site could bind two electrons and form a neutral open lattice site $(V_S 2-)2-$. See Van Gool (G_3).

An impurity centre in the atomic notation is indicated with the position of the substituted atom as a subscript. Sodium incorporated on a gallium position is denoted by Na_{Ga}, substitutional iodine on a sulphur position as I_S. Ionisation of these centres lead to Na'_{Ga} and I'_S. This is understood by the following condiderations:
The incorporation of iodine from the gas-phase into the lattice can be expressed by the equation

$$1/2\, I_{2(g)} + V_S^{\cdot\cdot} \longrightarrow I_S^{\cdot\cdot} \qquad (4.11)$$

This means that we have a double negatively charged iodine atom. As a group VII element, iodine can not be present as a -2 ion and for that reason it may act as a donor.

$$I_S^{\cdot\cdot} \rightleftharpoons I'_S + e' \quad . \qquad (4.12)$$

Incorporation of sodium into the lattice is expressed by

$$Na_{(g)} + V_{Ga}^{\cdot\cdot\cdot} \longrightarrow Na_{Ga}^{\cdot\cdot\cdot} \quad , \qquad (4.13)$$

and an analogous reasoning shows that this impurity may function as acceptor.

$$Na_{Ga}^{\cdot\cdot\cdot} \rightleftharpoons Na'_{Ga} + h^{\cdot} \qquad (4.14)$$

Taking into account the quantities of sodium detected, and the high degree of compensation demonstrated by some of the crystals, simultaneous incorporation of iodine and sodium is expected with a ratio of iodine to sodium concentrations close to one.
A mutual increase in solubility of iodine and sodium in GaS is assumed, like it has been observed in ZnS by Kröger et.al. (K_7) and in CdS by Schäfer et.al (S_9). The effect of an acceptor in increasing the solubility of a donor can be seen from the following.

For the incorporation of iodine in the lattice we write:

$$I_{(g)} \rightleftharpoons I_S^* \qquad \text{with } K_1 = \frac{[I_S^*]}{[I_g]} , \tag{4.15}$$

and

$$I_S^* \rightleftharpoons I_S^{\cdot} + e' \quad \text{with } K_2 = \frac{[I_S^{\cdot}]}{[I_S^*]} \cdot n . \tag{4.16}$$

Combining these gives

$$[I_S^{\cdot}] \cdot n = K_1 K_2 \cdot [I_g] = C_1 . \tag{4.17}$$

Analogous equations can be given for the incorporation of Na:

$$Na_{(g)} \rightleftharpoons Na_{Ga}^* \qquad \text{with } K_3 = \frac{[Na_{Ga}^*]}{[Na_{(g)}]} , \tag{4.18}$$

and

$$Na_{Ga}^* \rightleftharpoons Na_{Ga}' + h^{\cdot} \quad \text{with } K_4 = \frac{[Na_{Ga}']}{[Na_{Ga}^*]} \cdot p , \tag{4.19}$$

which results in

$$[Na_{Ga}'] \cdot p = K_3 K_4 \cdot [Na_{(g)}] = C_2 . \tag{4.20}$$

The concentrations of electrons and holes obey the equation:

$$n \cdot p = K_i , \tag{4.21}$$

while the equation giving the neutrality condition is:

$$[I_S^{\cdot}] + p = [Na_{Ga}'] + n \tag{4.22}$$

Using these expressions the following relations can be derived:

$$\left[I_S^{\cdot}\right] = \left[\frac{\left(C_1 + \frac{C_1 \cdot C_2}{K_i}\right)}{\left(1 + \frac{K_i}{C_1}\right)}\right]^{1/2}, \qquad (4.23)$$

and

$$\left[Na_{Ga}^{'}\right] = \left[\frac{\left(C_2 + \frac{C_1 \cdot C_2}{K_i}\right)}{\left(1 + \frac{K_i}{C_2}\right)}\right]^{1/2}. \qquad (4.24)$$

It follows from (4.23) that incorporation of Na - increasing C_2 - enhances the solubility of the iodine (H_7).
In case $\left[I_S^{\cdot}\right]$ and $\left[Na_{Ga}^{'}\right]$ are present in considerable amounts, we eventually arrive in the region where

$$K_i \ll C_1 \quad \text{and} \quad K_i \ll C_2 ,$$

from which follows:

$$\left[I_S^{\cdot}\right] \approx \left[Na_{Ga}^{'}\right] \approx \left[\frac{C_1 \cdot C_2}{K_i}\right]^{1/2} \qquad (4.25)$$

This is the case of charge compensation, which also can be deduced from the neutrality condition, equation (4.22), under the assumption that the concentrations of holes and electrons can be neglected.

4.8. Model for *n*-type GaS

A model for both groups of *n*-type crystals will be presented in this section. This model takes into account the results obtained with the analytical detection techniques. In the following discussion we

assume incorporation of iodine and sodium with concentrations in the same order of magnitude, in accordance with the description given in in section 4.7.

The observation of two ionisation energies leads to the assumption that there are two donors simultaneously present in the crystals. These donors D_1 and D_2 have ionisation energies $E_{D1} \approx 0.85$ eV and $E_{D2} \approx 0.60$ eV and numbers N_{D1} and N_{D2} respectively. Furthermore we have acceptors A with a concentration N_A.

When the deeper lying donor D_1 manifest itself in the measurements, which is the case for the group I crystal, D_2 is fully ionized, and the statistical formula for $n = f(T)$, reads

$$\frac{n\,(N_A + n)}{(N_{D1} + N_{D2} - N_A - n)\,.\,N_C} = e^{-E_{D1}/kT} \qquad (4.26)$$

From the straight parts of the curves (see fig. 4.8) we now obtain information about E_{D1} and $(N_{D1} + N_{D2}) / N_A$ (compare equation 4.6) and we get:

$$\gamma_n - 1 = (n/N_C)\,.\,e^{E_{D1}/kT}\,, \qquad (4.27)$$

where

$$\gamma_n = \frac{N_{D1} + N_{D2}}{N_A}\,. \qquad (4.28)$$

FOR $N_{D2} \ll N_{D1}$, $\gamma_n \approx N_{D1}/N_A$. (4.29)

In the case that the deeper lying donor D_1 is fully occupied and D_2 is partly ionized, the number of electrons in the conduction band as a function of temperature is given by

$$\frac{n(N_A + n)}{(N_{D2}-N_A-n).\ N_C} = e^{-E_{D2}/kT} \quad , \tag{4.30}$$

which leads to

$$\gamma_n - 1 = (n/N_C) \quad e^{E_{D2}/kT} \quad , \tag{4.31}$$

with $$\gamma_n = N_{D2}/N_A \quad . \tag{4.32}$$

We will identify acceptor A, (concentration N_A) with sodium and the donor D_1, (having a concentration N_{D1}) with iodine. We assume also $N_{D1} \approx N_A$.
This means that the number of acceptors N_A in the group I crystals will be $\approx$ 3.5 x $10^{19}/cm^3$; which is the detected amount of sodium; see table 4-II. Using the values of γ_n as given in the table, the value of $N_{D1} + N_{D2}$ can be calculated from equation (4.28).
For the group II crystals the number of relevant donors is N_{D2} and that of the relevant acceptors is N_A. From the position of the exhausted range $N_{D2} - N_A$ in fig. 4.8 it can be deduced that these numbers are of the order of 10^{16} / cm^3.
Using equation 4.32 and the estimated $N_{D2} - N_A$ values for the various crystals we are able to evaluate N_{D2} and N_A.
Table 4-III summarizes the results for the two groups of crystals based on the considerations given above. In the compiling of this table it is assumed that in the group I crystals, the fully ionized donor D_2 is present in amounts ($\approx 10^{16}$ / cm^3) equal to that in the group II crystals and that the fully occupied donor D_1, is present in group II crystals in amounts of the same order of magnitude ($\approx 10^{16}/cm^3$) as the acceptors Na.

An important result which emerges from the data is the fact that the crystals of group II contain less impurities than those of group I. This suggests that our attempts to produce purer crystals have not been un-

TABLE 4-III

Values of the acceptor concentrations N_A, the donor concentrations N_{D_1} and N_{D_2} and the exhausted ranges $N_{D_1} - N_A$ and $N_{D_2} - N_A$ for crystals of group I and group II

crystal	S_4	S_7	S_8	S_{16}	S_{13}	S_{21}	S_{25}	S_{27}	S_{41}	S_{43}	S_{44}	S_{45}	S_{51}
N_A (cm^{-3}) (detected)	$3.5.10^{19}$ *)	$3.5.10^{19}$ *)	$3.5.10^{19}$ *)	$3.5.10^{19}$ *)	$1.8.10^{18}$ †)	$1.8.10^{18}$ †)	-	-	-	-	-	-	-
N_A (cm^{-3}) (calculated)	-	-	-	-	-	-	4.10^{16}	4.10^{17}	3.10^{16}	4.10^{16}	2.10^{16}	6.10^{16}	2.10^{16}
E_{D_1} (eV)	0.85	0.82	0.83	0.85	(~ 0.8)	~ 0.8	~ 0.8	~ 0.8	~ 0.8	~ 0.8	~ 0.8	~ 0.8	~ 0.8
$N_{D_1} = [I_S]$ (cm^{-3})	$3.8.10^{19}$	$5.2.10^{19}$	$3.7.10^{19}$	$6.8.10^{19}$	-	-	~ 10^{16}	~ 10^{16}	~ 10^{16}	~ 10^{16}	~ 10^{16}	~ 10^{16}	~ 10^{16}
E_{D_2} (eV)	~ 0.6	~ 0.6	~ 0.6	~ 0.6	0.52	0.66	0.50	0.57	0.57	0.57	0.57	-	0.63
$N_{D_2} = [V_S]$ (cm^{-3})	~ 10^{16}	~ 10^{16}	~ 10^{16}	~ 10^{16}	-	-	5.10^{16}	8.10^{16}	5.10^{16}	8.10^{16}	6.10^{16}	10^{17}	7.10^{16}
$N_{D_1} - N_A$ (cm^{-3}) (calculated)	$3.0.10^{18}$	$1.7.10^{19}$	$2.0.10^{18}$	$3.3.10^{19}$	-	-	-	-	-	-	-	-	-
$N_{D_2} - N_A$ (cm^{-3}) (estimated)	-	-	-	-	-	-	10^{16}	4.10^{16}	2.10^{16}	4.10^{16}	5.10^{16}	5.10^{16}	5.10^{16}
group	I				II								

*) spectrochemical analyses obtained from Dr. N.W.H. Addink.

†) Neution activation data obtained from Dr. H.A. Das

succesful. The behaviour of S_{13} is rather odd, as can be seen in fig. 4.8. This crystal will therefore not be taken into consideration for further discussions.

Regarding the measurements of S_{21} it may be noted that the value of $1.8.10^{18}/cm^3$ for $[Na] = N_A$, as well as the activation energy, $E_{D2} = 0.66$ eV lie in between the values for the main groups. It is very probable that the purity also lies in between those of group I and II. For S_{25} and S_{27} there are no analytical data available, neither is it possible to estimate N_{D2}-N_A values. However the measurements in fig. 4.8 show these two crystals to be comparable with S_{43}.

In fig. 4.13 the theoretical curves for $n = f(10^3/T)$ based on the statistical formulae and on the characteristic values for the various parameters, as given in table 4-III are presented by dotted lines.

For group I crystals the constant values of n are reached at temperatures beyond the range of our measurements. For the group II samples the lines are given for S_{43} and S_{51} only to avoid confusion on account of the number of curves. The strong increase of the electron concentration of S_{43} is probably due to surface diffusion.

In the model described, we are left with the question of the identity of the donor D_2,

Referring to section 4.7 we might expect that sulphur vacancies function as donors and are present in concentrations $\approx 10^{17}/cm^3$, exceeding that of the gallium vacancies. Otherwise, these gallium vacancies have to be included in the statistical calculations as an extra acceptor. The band picture derived from these results is given in fig. 4.14a and b. When n is neglected in the expression for the electroneutrality, the approximate position of E_F (the difference in electronic energy between the bottom of the conduction band and the position of the Fermi level, see the footnote on page 80) can be found from (4.27) and (4.31).

$$E_F = E_{D1,2} - kT \ln (\gamma_n - 1) \qquad (4.33)$$

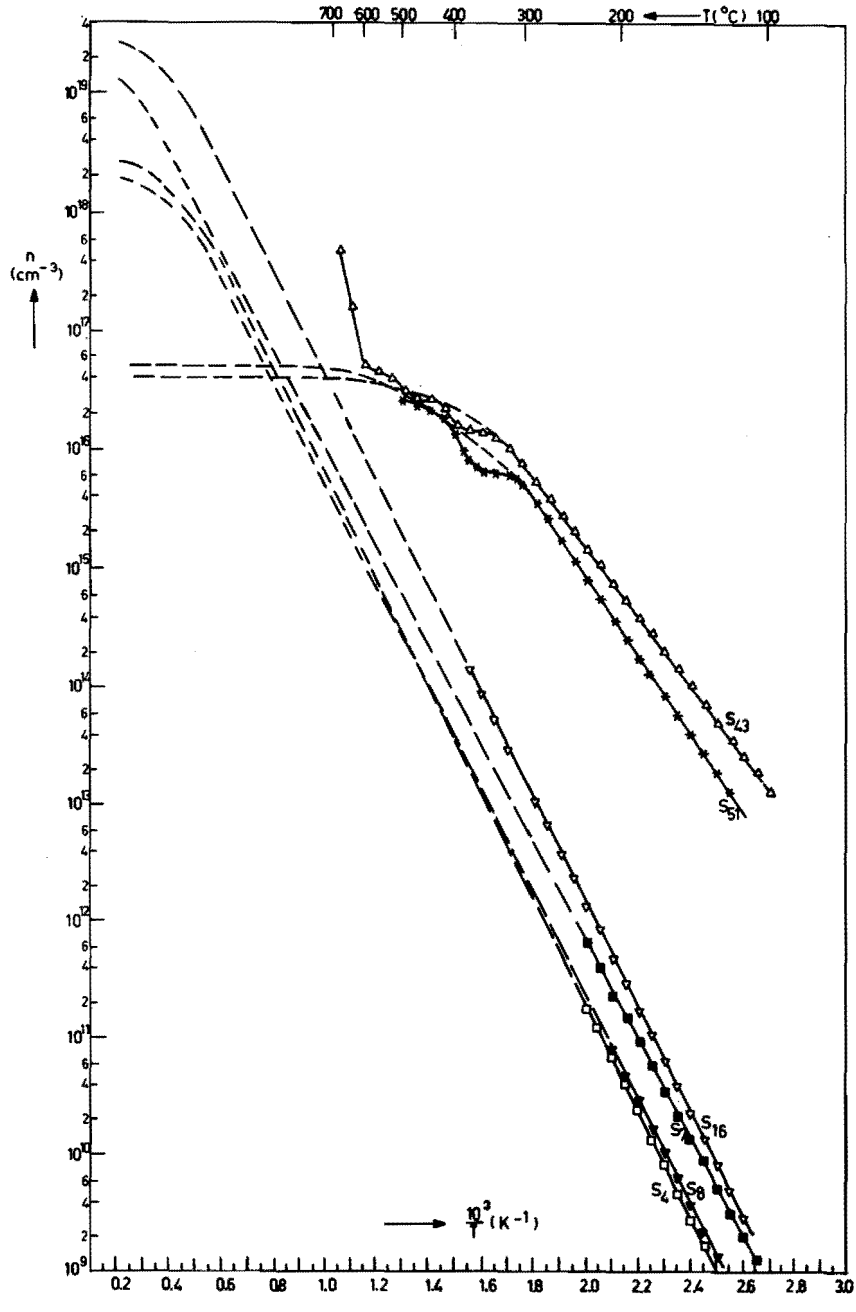

Fig. 4.13. Concentration (n) of free electrons versus $10^3/T$ with the calculated exhausted ranges for S_4, S_7, S_8, S_{16}, S_{43} and S_{51}.

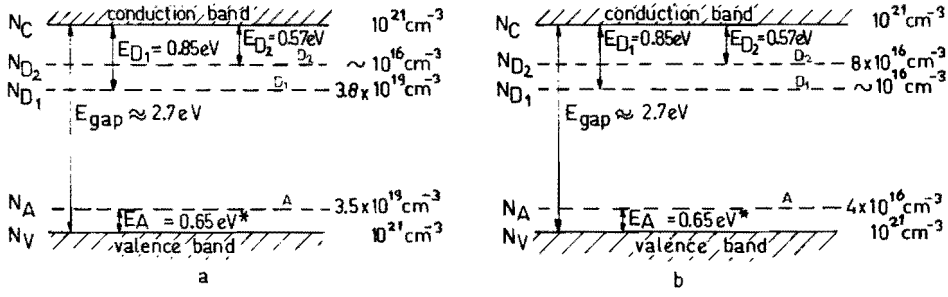

Fig. 4.14. Band picture for n-type crystals, a) for crystal S_4, (b) for crystal S_{43}. The donor D_1 stands for I_S, donor D_2 stands for V_S and acceptor A stands for Na_{Ga}.
(*) The value of 0.65 eV is obtained from analysis of p-type crystals.

For S_{43}, at roomtemperature, $E_F = E_{D2}$, for S_{51}, E_F lies 0.02 eV above E_{D2}. For samples with a high degree of compensation, like S_4 and S_8, E_F lies 0.06 eV below E_{D1} at roomtemperature.

4.9. Results for *p*-type crystals.

In fig. 4.15 the dark specific conductivity versus reciprocal temperature is presented for two sorts of *p*-type crystals. Those denoted S_2 and S_5 belong to one group, are produced by the sublimation technique and are from different batches. The polycrystalline starting material was prepared without a boat. Sample S_{20} on the other hand was sublimation-grown from starting material that was synthesized in an alumina boat.
The activation energies ε for the conductivity are given in table 4-IV together with the avarage values of the ratio R_1/R_2 (see section 4.4)

For the temperature dependence of the Hall mobility of *p*-type GaS, Kipperman and Vermij (K_8, V_1) found the relation

$$u_{Hp} = 12.(T/300)^{-2.4} \ cm^2/Vs \ . \qquad (4.34)$$

Using u_{Hp}, the concentration of free holes p, as a function of $10^3/T$, can now be calculated for the three crystals. The results are given in fig. 4.16. From the slopes, two different activation energies can be calculated: for S_2 and S_5 an energy E_A = 0.65 eV is found, while for S_{20}, E_A = 0.90 eV.

TABLE 4-IV

activation energy ε of the conductivity and average values of R_1/R_2

crystal	S_2	S_5	S_{20}
ε (eV)	0.57	0.59	0.83
average R_1/R_2	3.0	1.3	2.8

Using a compensated model for these samples the ratio $\delta_p = N_A/N_D$ can be calculated in an analogous way as performed in section 4.6, for the n-type crystals. For N_V - the density of states in the valence band - a value of $10^{21}/cm^3$ as found by Kipperman and Sliepenbeek (K_9, S_8), was taken. It must be admitted that nothing definite can be said about the compensating donor; it seems probable however that this role is played by sulphur vacancies. The data found are presented in table 4-V together with results from spectrochemical and neutron activation analyses regarding the concentration of incorporated sodium [Na].

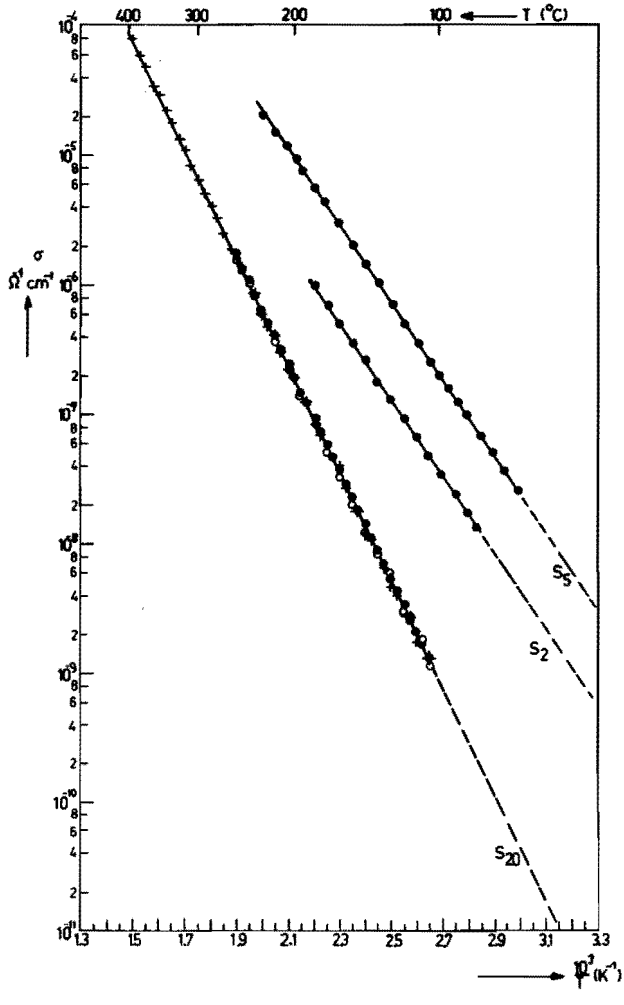

Fig. 4.15. Conductivity (σ) versus $10^3/T$ of the p-type crystals S_2, S_5 and S_{20}. The heating and cooling cycle for S_{20} is: heated to 250° (o), cooled to room temperature (•) and heated to 400°C (+).

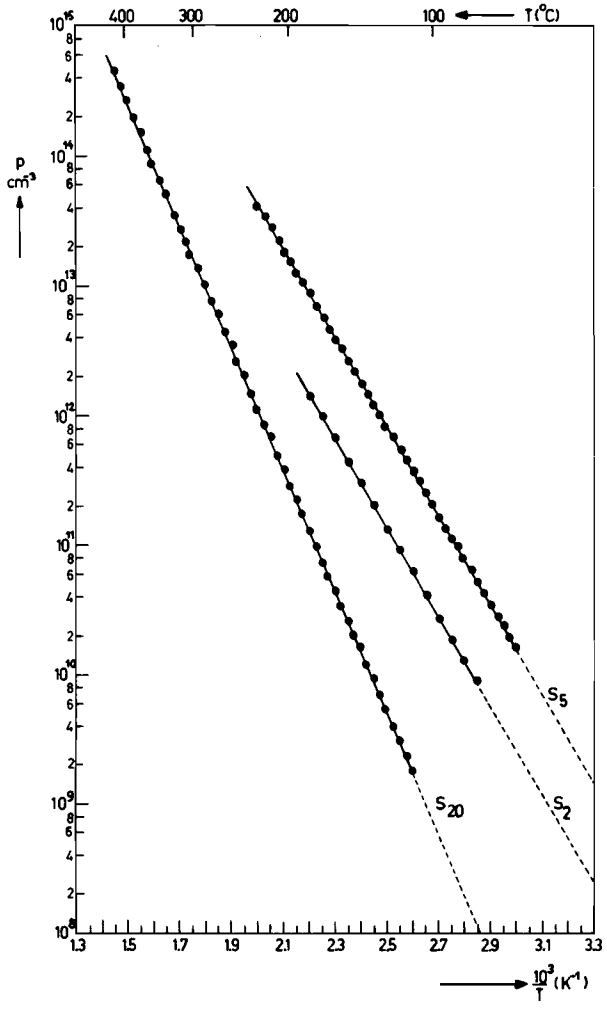

Fig. 4.16. Concentration (p) of free holes versus $10^3/T$ of the p-type crystals S_2, S_5 and S_{20}.

TABLE 4-V

The ionisation energy of acceptors (E_A) and the ratio γ_p for the crystals S_2, S_5 and S_{20}

crystal	S_2	S_5	S_{20}
E_A (eV)	0.65	0.65	0.90
$\gamma_p = N_A/N_D$	1.05	1.30	2.64
[Na] cm^{-3}	$2.5.10^{19}$ *)	$2.5.10^{19}$ *)	$3.6.10^{17}$ †)

*) Spectrochemical data obtained from Dr. N.W.H. Addink

†) Neutron activation analyses obtained from Dr. H.A. Das

4.10 Interpretation of the results for *p*-type crystals

In the *p*-type crystals, the iodine is absent as is discussed in chapter 3. According to table 4-V the interpretation for the *p*-type crystals requires two types of acceptors A_1 and A_2 with activation energies E_{A1} = 0.65 eV and E_{A2} = 0.90 eV respectively.
According to the description given in section 4.7 the following identification of the defects can be proposed:

donor D: sulphur vacancies with a concentration N_D and ionisation energy E_D = 0.57 eV *).

acceptor A_1: incorporated sodium with a concentration N_{A1} and ionisation energy E_{A1} = 0.65 eV.

acceptor A_2: gallium vacancies with a concentration N_{A2} and ionisation energy E_{A2} = 0.90 eV.

*) This value is obtained from the analyses of n-type crystals.

The sodium concentration $[Na] = N_{A1}$ is found from analyses; for crystals S_2 and S_5, $N_{A1} = 2.5.10^{19}/cm^3$, for crystal S_{20} a value of $3.6.10^{17}/cm^3$ is found for N_{A1}. The conductivity of S_2 and S_5 is thought to be caused mainly by ionisation of the sodium; in reducing the concentration of this impurity however - like in S_{20} - it is assumed that the concentration of the metal vacancies will outweight that of the sodium and hence replace the sodium as the prominent acceptor. It is resonable to expect a deep level for $V_{Ga}^{''}$ and we expect this vacancy acceptor to ly further from the valence band than the sodium-acceptor.

If the vacancies of gallium and sulphur occur in equal numbers, then the concentration $[V_{Ga}^{''}] = [V_S^{\cdot\cdot}]$ is related to the energy associated with the formation of a set of vacancies by the expression:

$$[V_{Ga}^{''}] = [V_S^{\cdot\cdot}] = N.\, e^{-\Delta H_f/2kT} \,.\, e^{T\ \Delta S_v/2kT} \approx N.\, e^{-E_S/2kT} \qquad (4.35)$$

for $[V_{Ga}^{''}] \ll N.$ (M4)

Here N is the number of GaS molecules per cm^3, ΔH_f is the enthalpy of formation of such a set and ΔS_v is the vibrational entropy resulting from the disturbance of nearest neighbours.

Taking $E_S = 2$ eV and $N = 2.10^{22}/cm^3$ we find from (4.35) at 900°C:

$$[V_S^{\cdot\cdot}] = [V_{Ga}^{''}] \approx 10^{18}/cm^3 \quad . \qquad (4.36)$$

The constant K_S is therefore

$$K_S = [V_S^{\cdot\cdot}] \,.\, [V_{Ga}^{''}] = 10^{36}/cm^6 \quad . \qquad (4.37)$$

The evaluation of the electrical measurements can be performed in an analogous way as done for the n-type samples. Hence for S_2 and S_5 the donor concentrations N_D can be obtained from $\gamma_p = N_{A1}/N_D$. They are of the same order of magnitude as $N_{A1} \approx 10^{19}/cm^3$.

The number N_{A2} which is not detected in the electrical measurements of S_2 and S_5 is probably low, $< 10^{18}/cm^3$, due to the incorporation of the considerable amount of sodium.
For the crystal S_{20} the following must be considered:

$$\left[V_{Ga}^{\prime\prime\prime}\right] \quad \left[V_S^{\cdot\cdot}\right] = N_D \cdot N_{A2} = 10^{36}/cm^6,$$

as given in equation (4.37).

Furthermore from the measurements we have

$$\gamma_p = \frac{N_{A1} + N_{A2}}{N_D} = 2.64 \qquad (4.38)$$

Since $N_{A1} = [Na]$, is known to be $3.6.10^{17}/cm^3$, we obtain from (4.37) and (4.38):

$$N_D = 7.10^{17}/cm^3 = \left[V_S^{\cdot\cdot}\right]$$

and

$$N_{A2} = 1.5.10^{18}/cm^3 = \left[V_{Ga}^{\prime\prime\prime}\right]$$

The values of the various parameters are collected in table 4-VI for the three crystals. The values of N_D, N_{A1} and N_{A2} give an indication of the position of the exhausted regions.
Fig. 4.17 shows the curves of $p = f(10^3/T)$. It is seen that the calculated exhausted range is reached at temperatures in the neighbourhood of the melting point of the compound.
In fig. 4.18 a and b the bandschemes are given. The results, regarding the donor energy E_D from the analyses of the *n*-type crystals, are included.

TABLE 4-VI

The concentrations of acceptors N_{A1} and N_{A2}, of the compensating donor N_D and the exhausted range $(N_{A1}-N_D)$ and $(N_{A1}+N_{A2}-N_D)$ for p-type crystals.

crystal	S_2	S_5	S_{20}
E_{A1} (eV)	0.65	0.65	0.65
$N_{A1}=[Na]$ (cm^{-3}) (detected)	$2.5.10^{19}$ *)	$2.5.10^{19}$ *)	$3.6.10^{17}$ †)
E_{A2} (eV)	$\sim$ 0.90	$\sim$ 0.90	$\sim$ 0.90
$N_{A2}=[V_{Ga}^{'''}]$ (cm^{-3})	$< 10^{18}$	$< 10^{18}$	$1.5.10^{18}$
$N_D=[V_S^{\cdot\cdot}]$ (cm^{-3})	$2.4.10^{19}$	$1.9.10^{19}$	7.10^{17}
$N_{A1}-N_D$ (cm^{-3}) (calculated)	10^{18}	6.10^{18}	–
$N_{A1}+N_{A2}-N_D$ (cm^{-3}) (calculated)	–	–	$1.2.10^{18}$

*) Spectrochemical analyses from Dr. N.W.H. Addink

†) Neutron activation data from Dr. H.A. Das

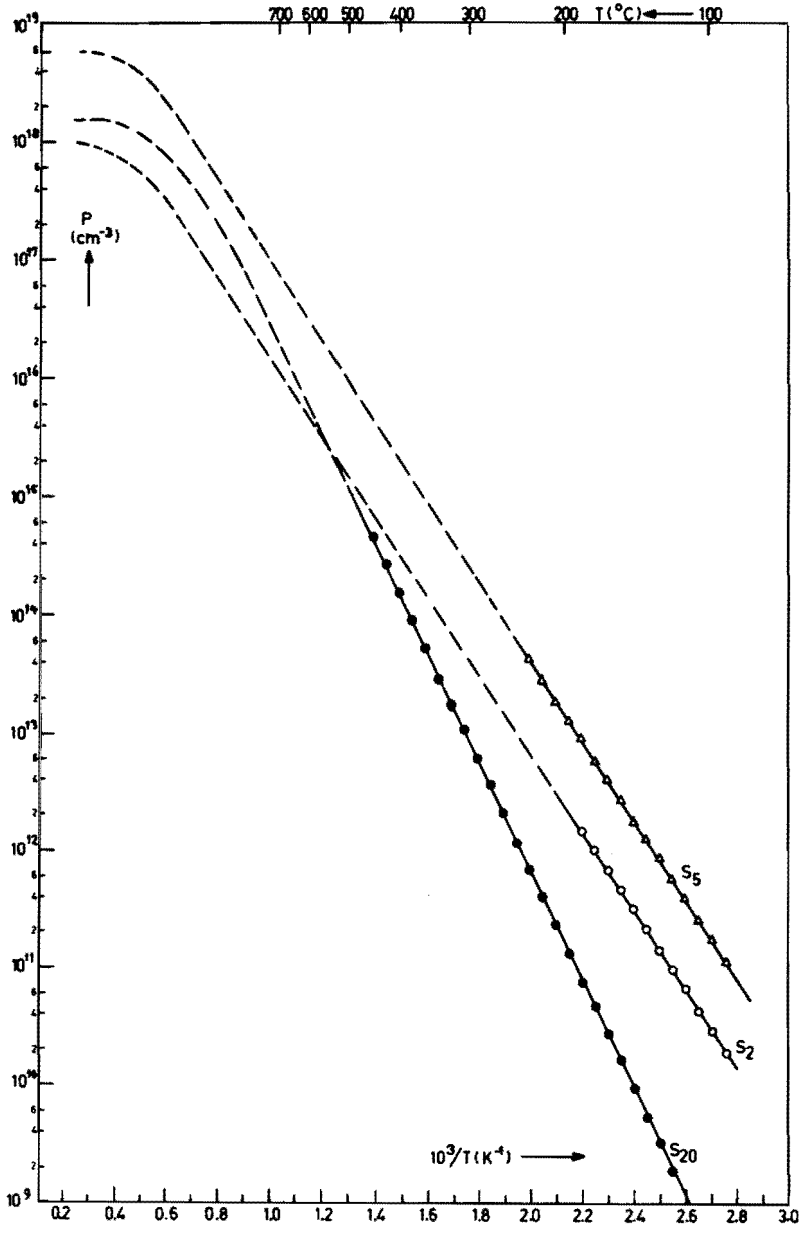

Fig. 4.17. Concentration (p) of free holes versus $10^3/T$ with the calculated exhausted ranges for S_2, S_5 and S_{20}.

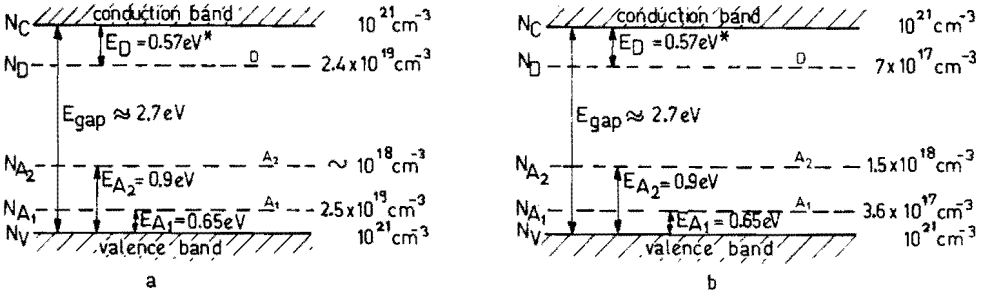

Fig. 4.18. Band-picture of p-type crystals, (a) for S_2 (b) for S_{20}. The acceptor A_1 stands for Na_{Ga}, acceptor A_2 stands for V_{Ga} and donor D stands for V_S.
(*) The value of 0.57 eV is obtained from analysis of n-type crystals.

When p is neglected in the expression for the electroneutrality, the approximate position of E_F can be found from

$$E_F = E_{A1,2} - kT \ln (\gamma_p - 1) \qquad (4.39)$$

For S_{20} at roomtemperature E_F lies 0,01 eV below E_{A2}, for S_2, E_F lies 0.08 eV above E_{A1} and for S_5, E_F lies 0.03 above E_{A1}.

4.11 Conclusions

The arrangement used in the measurements of the conductivity versus temperature has proved to be satisfactory. Although there exists no information about the selfdiffusion of gallium in gallium sulphide, to us gallium seemed prefarable to other metalelectrodes.
This on account of the fact that the self diffusion of gallium is expected to be small.

Both the n- as well as the p-type crystals can be divided into two main groups. The earliest produced samples contain a higher sodium concentration than the more recently produced crystals; the difference is about $10^3/cm^3$

For the *n*-type crystals the proposed model contains two donors and one acceptor, it is assumed that iodine is the dominant donor in the earliest types while sulphur vacancies are expected to be the dominant donor in the purer samples.

The proposed model for the *p*-type samples works with two acceptors and one donor. In the earliest samples the sodium is expected to be dominant, reducing the concentration of this impurity changes the type of acceptor. Gallium vacancies are probably the dominant acceptors in the purer crystal.

As mentioned in the last part of this chapter, we have restricted ourselves to the most plausible native defects - like gallium and sulphur vacancies - and to the incorporated impurities sodium and iodine. It must be stressed however that the existence of a more complicated model belongs to the possibilities.

Some crystals received a heat treatment at about 400°C; the rate of the subsequent cooling has an effect on the conductivity. In the present state of our investigations we can not offer an explanation for it, it is probably due to atomic interactions, like the dissociation of associated pairs or even of clusters.

Final remarks

The work described in this thesis has shown that we are still a long way off from material with a purity as for example can be achieved in compounds like CdS and ZnS.
Sensitive analytical detection methods combined with a purification technique like zone-refining can be helpful tools in future attempts to suppress the impurity content in GaS. Closely related to such work are investigations of the solubility of foreign elements in this compound; again in combination with purification techniques and associated with advanced methods of chemical analyses.

Another point of interest is the diffusion, however experiments to investigate selfdiffusion and the diffusion of foreign atoms do not seem to be easy to devise, owing to the layer structure.
The problems encountered in doping gallium sulphide, related for example to the solubility, have already at the moment received full attention of Mr. G.A. van der Leeden of our physics Department.

We are left with the question about the detection of the incorporated iodine. We hope to be able to intensify the efforts to determine the concentration of this impurity.

Regarding the results of our heat treatments, it must be emphasized that the investigations are far from exhausted and it seems important to combine future work in this direction with experiments on luminescence.

REFERENCES

A_1 G.A. AKHUNDOV and T.G. KERIMOVA, Phys. Stat. Sol. Vol. 16, K 15, (1966).

A_2 G.A. AKHUNDOV, N.A. GASANOVA and M.A. NIZAMETDINOVA, Phys. Stat. Sol. Vol. 15, K 109, (1966).

A_3 W. ALBERS and K. SCHOL, Philips Res. Repts. Vol. 16, 329, (1961).

B_1 A. BRUKL und G. ORTNER, Naturwiss. Vol. 18, 393, (1930); Monatshefte Vol. 56, 358, (1930).

B_2 J.L. BREBNER and G. FISCHER, International Conference on the Physics of Semiconductors, Exeter 1962, pp 760.

B_3 J.L. BREBNER, Helv. Phys. Acta, Vol. 37, 589, (1964).

B_4 R.H. BUBE and E.L. LIND, Phys. Rev. Vol. 119, 1535, (1960).

B_5 J.L. BREBNER, 7th International Conference on the Physics of Semiconductors, Paris 1964, pp 239.

B_6 J.L. BREBNER, G. FISCHER and E. MOOSER, J. Phys. Chem. Solids, Vol. 23, 1417, (1963).

B_7 J.M. VAN DEN BERG, Thesis, Leiden 1964.

B_8 J. BLOEM, Thesis, Utrecht 1956.

C_1 C.N. COCHRAN and L.M. FOSTER, J. Electrochem. Soc. Vol. 109, 149, (1962).

C_2 C.N. COCHRAN and L.M. FOSTER, J. Electrochem, Soc. Vol. 109, 144, (1962).

D_1 I. DEV and R.B. LAUER, Mat. Res. Bull. Vol. 185, (1966).

D_2 H.J. VAN DAAL, Thesis, Amsterdam 1964.

D_3 J. DIELEMAN, J.W. de JONG and T. MEYER, J. Chem. Phys. Vol. 45, no. 9, 3178, (1966)

F_1 G. FISCHER and J.L. BREBNER, J. Phys. Chem. Solids Vol. 23, 1363, (1962).

F_2 G. FISCHER, D. GREIG and E. MOOSER, Rev. Sci. Instr. Vol. 32, no. 7, 842, (1961).

G_1 E.G. GROCHOWSKI, D.R. MASON, G.A. SCHMIDT and P.H. SMITH, J. Phys. Chem. Solids Vol. 25, 551, (1964).

G_2 E.F. GROSS, B.V. NOVIKOV, B.S. RAZBIZIN and L.G. SUSLINA, Optics and Spectroscopy Vol. 4, 364, (1959).

G_3 W. van GOOL, Principles of Defect Chemistry of crystalline Solids, Academic Press, New York, London, 1966, pg. 19

H_1 H. HAHN und G. FRANK, Z. anorg.u. allgem. Chemie Bd. 278, 340, (1955).

H_2 M. HANSEN, Constitution of Binary alloys, Metallurgy and Metallurgical Engineering Series, McGraw-Hill Book Co., New York, Toronto, London 1958.

H_3 H. HAHN, Z. angew. Chemie 65 Jahrg. no. 21, 538, (1953).

H_4 W. HUME-ROTHERY, J.W. CHRISTIAN and W.B. PEARSON, Metallurgical Equilibrium Diagrams, Chapman and Hall, London, 1953.

H_5 H.J.M. HEYLIGERS, T.H.E. Report on crystal growth experiments. (in Dutch).

H_6 H.J.M. HEYLIGERS, Afstudeerverslag, T.H. Eindhoven 1967.

H_7 N.B. HANNAY, Solid State Chemistry, Prentice-Hall Inc., 1967.

I_1 F.I. ISMAILOV, E.S. GUSEINOVA and G.A. AKHUNDOV, Sovj. Phys. Sol. States Vol. 5, 2656, (1964).

J_1 K. JELLINEK und A. DEUBEL, Z. Electrochem.u.angew. phys. Chem. Vol. 35, 451, (1929).

K_1 W. KLEMM und H.U. Von VOGEL, Z.anorg.u.allgem. Chem. Bd. 219, 45, (1934).

K_2 A.H.M. KIPPERMAN and G.A. VAN DER LEEDEN, Solid State Comm. Vol. 6, 657, (1968).

K_3 H. KAMIMURA, J. Phys. Soc. Japan Vol. 24, 1313, (1968).

K_4 O. KUBASCHEWSKI and E.L.L. EVANS, Metallurgical thermochemistry, Oxford Pergamon Press, 1958.

K_5 F.A. KRÖGER, The Chemistry of Imperfect crystals, North-Holland Publ., Amsterdam, 1964.

K_6 F.A. KRÖGER and H.J. VINK, Solid State Phys. Vol. 3,307, (1956).

K_7 F.A. KRÖGER, H.J. VINK and J. VAN DEN BOOMGAARD, Z. Phys. Chemie Bd. 203, 1, (1954).

K_8 A.H.M. KIPPERMAN and C.J. VERMIJ, to be published in Il Nuovo Cimento.

K_9 A.H.M. KIPPERMAN and T.B.A.M. SLIEPENBEEK, to be published in Il Nuovo Cimento.

L_1 R.M.A. LIETH, H.J.M. LEIJLIGERS and C.W.M. VAN DER HEIJDEN, J. Electrochem. Soc. Vol. 113, no. 8, 798, (1966).

L_2 LANDOLT-BÖRNSTEIN, Zahlenwerte und Funktionen (aus Physik, Chemie, Astronomie), Springer-Verlag, Berlin-Göttingen-Heidelberg 1960.

L_3 W.M. LATIMER, J. Amer. Chem. Soc. Vol. 73, 1480, (1951).

L_4 G. VAN DER LEEDEN, Afstudeerverslag, T.H. Eindhoven 1967.

M_1 J.F. MILLER, Compound Semiconductors Vol. 1, pp 203, Reinhold Publ. Corp. Ltd., London.

M_2 B.J. MASON, The art and Science of growing crystals, (editor Gilman), John Wiley and Sons, New York, London, 1963.

M_3 E. MOOSER, Private Communication.

M_4 N.F. MOTT and R.W. GURNEY, Electronic processes in ionic crystals, at the Clarendon - press, 1948.

N_1 P.C. NEWMAN, J.C. BRICE and H.C. WRIGHT, Philips Res. Repts. Vol. 16, 41, (1961).

N_2 R. NITSCHE, H.U. BÖLSTERLI and M. LICHTENSTEIGER, J. Phys. Chem. Solids Vol. 21, 199, (1961).

N_3 M.A. NIZAMETDINOVA, Phys. Stat. Sol. Vol. 19, K 111, (1967).

P_1 L.S. PALATNIK and E.K. BELOVA, Inorg. Materials Vol. 2, 657, (1966).

P_2 L.J. VAN DER PAUW, Philips Res. Repts. Vol. 13, 1, (1958).

P_3 E.H. PUTLEY, The Hall effect and related phenomena, Butterworths, London, 1960.

R_1 P.G. RUSTAMOV, A.D. MELIKOVA, M.G. SAFAROV and M.A. ALIDZHANOV, Inorg. Materials Vol. 1, 387, (1965).

R_2 M. RANDALL and F.R. VON BICKOWSKY, J. Amer. Chem. Soc. Vol. 40,368, (1918).

R_3 R.F. ROLSTEN, Iodide metals and metal iodides, John Wiley and Sons, New York 1961.

S_1 N. SPANDAU and F. KLANBERG, Z.anorg.u.allgem. Chem. Bd. 295, 300, (1958).

S_2 G.K. SLAVNOVA, N.P. LUZHNAYA and Z.S. MEDVEDESVA, Zhur. Neorganicheskoi Khim Vol. 8, 1199, (1963).

S_3 K. SCHUBERT, E. DÖRRE und M. KLUGE, Z. Metallkunde Bd 46, heft 3, 216, (1955).

S_4 D.R. STULL and G.C. SINKE, Thermodynamic properties of the elements, Adv. Chem. - Series (18), 1962.

S_5 R.A. SWALIN, Thermodynamics of Solids, John Wiley and Sons, New York, London, 1962.

S_6 H. SCHÄFER, Chemische Transportreaktionen, Verlag Chemie, 1962.

S_7 I.A. SHEKA, I.S. CHAUS and T.T. MITYUREUA, The Chemistry of Gallium, Elsevier Pub. Co., Amsterdam, 1966.

S_8 T.B.A.M. SLIEPENBEEK, Afstudeerverslag, T.H. Eindhoven 1968.

S_9 H. SCHÄFER und H. ODENBACH, Z. anorg.u.allgem.Chem. Bd. 346, 127, (1966).

S_{10} F. STÖBER,(cited by H.E.Buckley (ed)) in Crystal growth, John Wiley and Sons, 1961, p.p. 89.

S_{11} H. SAMELSON, J. App. Phys. Vol. 32, 309 (1961).

V_1 C.J. VERMIJ, Afstudeerverslag, T.H. Eindhoven 1968.

Summary

In this thesis some physico-chemical properties of gallium sulphide are investigated and attention is paid to the impurity concentration in our materials, so that we could try to find better preparation techniques. Furthermore, the influence of temperature on the conductivity of *n*- and *p*-type single crystals are studied.

In chapter 1 a survey of the literature on GaS is presented. The earliest articles describe the preparation of the compound from the elements and the determination of the crystal structure. More recently much research has been directed to physical properties like optical absorption and photoconductivity but the influence of temperature on the conductivity is scarcely mentioned.

In chapter 2 a describtion is given of the way in which gallium sulphide is prepared and the precautions taken to suppress the impurity content. A comparative presentation of the concentration of foreign atoms in the polycrystalline solid and in its components is given. Furthermore the relations between pressure, temperature and composition are studied. It shows that there are two compounds in the system gallium-sulphur i.e. GaS and Ga_2S_3 with melting points of 962° and 1090°C respectively. The partial sulphur pressure above GaS is low, the p_{S_2} is $2.2.10^{-4}$ mmHg at the melting point. The partial sulphur pressure of Ga_2S_3 is 1.8 mmHg at the melting point. On the other hand p_{GaS} is higher, it is 4 mmHg at the melting point of GaS. This is of importance for experiments with crystals; at higher temperatures sublimation of the crystal can occur. An interesting fact is that the range of homogeneity of GaS lies on the sulphur rich side. Investigations at elevated temperatures have proved the compound to be stable.

In chapter 3, the preparation of single crystals is described. Three methods are discussed.
The easiest method which produces the largest crystals in the shortest time is the iodine transport process. The crystals contain some iodine and show an *n*-type conductivity. Crystals produced by sublimation are iodine free and show *p*-type conductivity. However the yield

of useful crystals is very low. Growth from the melt produces ingots from which samples can be cut which also show *p*-type conductivity. A comparative presentation of the impurity concentration in the monocrystalline compound, prepared by the different techniques. is given for both *n*- and *p*-type crystals.
Furthermore the differences observed in the crystal habit are discussed. It seems that the presence of iodine atoms favours growth perpendicular to the *c*-axis.
Attempts to obtain doped single crystals are described.

In chapter 4 the specific dark conductivity as a function of temperature is discussed for both *n*- and *p*-type crystals. The method of Van der Pauw for measurements on plan-paralell crystals of arbitrary shape is used. As to the choice of the electrode material, this proved to be difficult. Early measurements were performed with alloyed indium contacts; they had no mechanical strength and caused much troubles at elevated temperatures. The majority of the experiments however were carried out with liquid gallium electrodes; the weight of a quartz plate presses the crystal into the four gallium pellets. This rather simple set-up functions very good.

The conductivity and the free electron concentration versus reciprocal temperature are presented for two groups of *n-type* crystals. Applying semiconductor statistics and taking into account the detected amounts of sodium, an attempt is made to construct a model for the *n*-type crystals. This model contains two donors and one acceptor. For the samples where analytical data about the sodium concentration were absent, use was made of an estimated exhausted range. The slopes of the electron concentration versus temperature curves for some *n*-type crystals, clearly indicate a tendence towards a range of constant concentration.
Confrontation of the model with the results of the measurements leads to values for the concentration of impurities which are of the order of $10^{19}/cm^3$ for the impure crystals and of the order of $10^{16}/cm^3$ for pure crystals.
For the *p*-type crystals a model with two acceptors and one donor is proposed.

A analogous reasoning as given for the *n*-type crystals leads for the *p*-type samples for the impurities to values of $10^{19}/cm^3$ in the case of the impure crystals and to $10^{17}/cm^3$ for the pure sample.
Regarding these results one can conclude that the attempts to produce purer crystals have not been unsuccesful.
For both *n*- and *p*-type crystals bandschemes have been proposed in which the values of the ionisation energies and the numbers of defects are indicated.
Some crystals received a heat treatment at 400-450°C; and the speed of cooling seems to be important. Very slowly cooled samples show an extra dip in their conductivity versus temperature curves which is not seen in the case of the quenched sample. In general such extra dips will not be seen, since ampouls used in the growth process are cooled at a rate which is fast compared to the very slow cooling discussed above. Those dips are probably due to atomic interactions, like the dissociation of associates or clusters.

The influence of the iodine concentration - used in the growth process - on the conductivity was investigated. It can be concluded that the conductivity becomes independent of the amount of iodine when the concentration exceeds a value of 2.5 mg/cm^3.

SAMENVATTING

I

In dit proefschrift worden enige fysisch-chemische eigenschappen van gallium sulfide onderzocht. Getracht werd om met behulp van analyses der onzuiverheden in het materiaal, tot betere bereidingsmethoden te komen. Daarnaast werd de temperatuur-afhankelijkheid van de specifieke donker geleiding van *n*- en *p-type* kristallen bestudeerd.

In hoofdstuk 1 wordt een overzicht gegeven van de bestaande literatuur. De oudste artikelen beschrijven de vervaardiging van de verbinding uit zijn componenten en voorts de bepaling van de kristalstructuur. Artikelen van recentere datum behandelen fysische eigenschappen zoals optische absorptie en fotogeleiding. Gegevens betreffende de invloed van de temperatuur op de donker geleiding zijn echter schaars.

In hoofdstuk 2 wordt een beschrijving gegeven van de bereiding van GaS en van de voorzorgen welke genomen worden om de concentratie der verontreinigingen zo laag mogelijk te houden. Er wordt een vergelijkend overzicht gegeven van de concentraties der vreemde atomen in de polykristallyne stof en in zijn componenten.
Voorts worden de relaties tussen de druk, de temperatuur en de samenstelling onderzocht. Er zijn twee verbindingen in het systeem galliumzwavel gevonden; GaS en Ga_2S_3 welke smeltpunten hebben van 962°C respectievelijk 1090°C.
De partiële zwavel druk boven GaS is laag, te weten $2{,}2.10^{-4}$/mm Hg bij 962°C. Boven Ga_2S_3 is de p_{S_2} = 1,8 mm Hg bij het smelpunt. De druk van het GaS daarentegen, p_{GaS}, is hoger, te weten 4 mm Hg bij 962°C. Voor experimenten met kristallen is dit van belang; bij hogere temperatuur kan sublimatie van het kristal optreden.
Van belang is voorts dat het gebied waar GaS homogeen is aan de zwavelrijke kant ligt. Overigens blijkt uit de experimenten bij hoge temperaturen, nl. rond het smeltpunt, dat de verbinding stabiel is.

In hoofdstuk 3 wordt de vervaardiging van één kristallen beschreven volgens twee fundamentele methodieken, namelijk groei uit de dampfase en groei uit een gesmolten fase. De methode waarbij gebruik wordt

gemaakt van jodium als transportmiddel - het jodium transport proces - is de meest eenvoudige wijze van werken, waarbij de grootste kristallen in de kortste tijd worden geproduceerd. Deze kristallen bevatten sporen jodium en geven een *n*-type geleiding te zien. Met behulp van sublimatie zijn jodium-vrije kristallen te verkrijgen, welke *p*-type geleiding vertonen. Groei uit de smelt levert brokken, waaruit éénkristallyne stukken te snijden zijn, welke eveneens *p*-type geleiding laten zien, doch welke het voordeel hebben dat ze dikker zijn. Een vergelijkend overzicht van de verontreinigingsgraad in de éénkristallen verkregen volgens de drie technieken, wordt gegeven. De kristalhabitus laat verschillen zien tussen kristallen welke met en zonder aanwezigheid van jodium gegroeid zijn. Het lijkt of de aanwezigheid van deze verontreiniging de groei loodrecht op de *c*-as van het kristal bevorderd.
Tenslotte worden de pogingen om gedoteerde éénkristallen te vervaardigen beschreven.

In hoofdstuk 4 wordt een overzicht gegeven van de specifieke donkergeleiding welke als functie van de temperatuur gemeten is, zowel aan *n*- als aan *p*-type kristallen. Hierbij wordt gebruik gemaakt van de methode van der Pauw voor het meten van plan-paralelle kristallen van willekeurige vorm. De keuze van goed kontakt materiaal was hierbij een grote moeilijkheid. Voor de eerste metingen werden gelegeerde indium contacten gebruikt welke bij hogere temperaturen instabiel werden en weinig of geen mechanische sterkte bezaten; de meerderheid der metingen werd met vloeibare gallium contacten uitgevoerd. Het gewicht van een kwarts dekplaatje drukt het kristal op de vier gallium bolletjes welke in de meethouder zijn aangebracht.
Deze zeer eenvoudige methode voldoet zeer goed. Voorts wordt van het meetcircuit dat voor hoogohmige monsters gebruikt wordt een schematisch overzicht gegeven.
Voor twee groepen van *n*-type kristallen wordt het geleidingsvermogen en de concentratie der vrije electronen - beiden als functie der temperatuur - gegeven.
Gebruik makend van de halfgeleider statistiek en mede aan de hand van de gedetecteerde hoeveelheden natrium is getracht een model op te

stellen voor *n-type* kristallen, waarbij twee donoren en een acceptor aanwezig zijn. Voor die kristallen waarvoor géén analytische gegevens omtrent de concentratie van het natrium voorhanden waren, is gebruik gemaakt van een - geschat - uitputtingsgebied. Bij enige *n*-type kristallen, is in het verloop van de electronen concentratie als functie van de temperatuur een tendens zichtbaar naar zo'n uitputtingsgebied. Confrontatie van het model met de meetresultaten leidt tot waarden van de concentraties der verontreinigingen welke voor de onzuivere kristallen van de orde van $10^{19}/cm^3$ zijn en voor de zuivere van de orde van $10^{16}/cm^3$.
Een analoge werkwijze is gevolgd voor de *p*-type kristallen waarbij in het model twee acceptoren en een donor veronderstelt zijn.
Analoog aan de beschouwingen als gegeven voor de *n*-type kristallen komt men tot de conclusie dat bij de onzuivere kristallen de concentraties van de orde van $10^{19}/cm^3$ zijn en bij het zuiverder kristal van de orde van $10^{17}/cm^3$.
Men zou mogen constateren dat de pogingen om tot zuiverder kristallen te komen enig succes hebben gehad.
Voor *n*- en *p*-type kristallen zijn tenslotte bandenschema's gegeven waarin de waarden van de activerings-energien en de aantallen defecten zijn aangegeven.
Enkele *n*-type kristallen werden voorts aan een warmte-behandeling op 400-450°C onderworpen. De snelheid van de daaropvolgende afkoeling blijkt van belang te zijn. Kristallen welke zeer langzaam werden gekoeld vertonen ongeacht hun voorgeschiedenis een extra knik in hun geleidingsvermogen welke bij de normaal- of snel-gekoelde kristallen ontbreekt. Het wordt waarschijnlijk geacht dat atomaire interacties zoals dissociaties van associaten of clusters de oorzaak zijn.
In het algemeen worden ampullen waarin het groeiproces plaats vindt gekoeld met een snelheid, welke groot is vergeleken bij de zeer langzame koeling welke in deze experimenten kan worden toegepast zodat daar extra knikken meestal niet gevonden worden.
De invloed van de hoeveelheid jodium - welke bij het groeiproces wordt gebruikt - op de geleiding is eveneens onderzocht. De geleiding blijkt bij hogere temperatuur onafhankelijk te worden van de hoeveelheid jodium, zodra deze een concentratie van 2,5 mg per cm^3 van het buisvolume overschrijdt.

CURRICULUM VITEA

Op verzoek van de Senaat der Technische Hogeschool volgen hier enkele persoonlijke gegevens.

Gedurende de oorlogsjaren werd in het voormalige Nederlands Indië zeer fragmentarisch Lager Onderwijs genoten. Het Middelbaar Onderwijs werd in 's-Gravenhage gevolgd, alwaar in 1951 het eindexamen H.B.S. werd afgelegd. In september van dat jaar volgde de inschrijving aan de R.U. te Leiden.
Het candidaats-examen F werd in juli 1955 afgelegd, waarna onmiddellijk mijn onmisbaarheid voor 's lands krijgsmacht duidelijk werd. Zodoende kon pas in april 1957 weer begonnen worden met de studie voor het doctoraal-examen.
Met ingang van september 1957 werd ik aangesteld tot assistent bij het anorganisch preparatief practicum.
Voor mijn bijvak kristallografie werd ik door het Reactor Centrum Nederland van september 1959 tot september 1960 in staat gesteld in Noorwegen bij het I.F.A. te Kjeller structuuronderzoek te verrichten.
In juni 1961 volgde het doctoraal-examen met hoofdvak anorganische chemie en bijvakken kristallografie en theoretische organische chemie.
Daarna was ik tot juli 1962 werkzaam bij de metallurgische groep van het I.F.A. Vanaf augustus 1962 ben ik in dienst van de Technische Hogeschool te Eindhoven.

DANKWOORD

Op de allereerste plaats wil ik beginnen mijn dankbaarheid uit te spreken tegenover mijn moeder die het mij mogelijk heeft gemaakt om te studeren. Voorts verdienen mijn dank al diegenen die op hun wijze hebben bijgedragen aan de totstandkoming van dit proefschrift. In het bijzonder wil ik mijn erkentelijkheid betuigen aan Ir. H.J.M. Heijligers en de heer C.W.M. van der Heijden voor het chemisch-preparatieve werk dat zij deden.

Zeer veel dank ben ik verschuldigd aan Ir. A.H.M. Kipperman en Ir. C. Vermij op wiens hulp ik altijd kon rekenen.
Hun kritische instelling bij discussies over physische problemen en hun nimmer aflatend enthousiasme en geduld om een chemicus het zinnig gebruik van electrische meetapparatuur bij te brengen zijn van onschatbare waarde geweest voor de geleidingsmetingen.
Voor de hulp bij de uitvoering van vele - zeer tijdrovende geleidingsmetingen - betuig ik gaarne mijn dank aan de heren J.W.M. van Kessel, A. van Meurs en C.W.M. van der Heijden. Zonder hun bijdrage was het niet mogelijk geweest nu reeds dit werk te presenteren.
Tot slot gaat mijn dank uit naar mijn echtgenote die onuitsprekelijk veel geduld heeft getoond en zich veel zorg heeft getroost voor de nodige huiselijke rust.

STELLINGEN

Behorende bij het proefschrift
van R.M.A. Lieth.
14 oktober 1969.

STELLINGEN

I

De door Spandau en Klanberg gevonden verbinding Ga_4S_5 bestaat niet.

H. Spandau und F. Klanberg, Z. anorg. u. allgem. Chem. Bd. 295, 300, 1958.
Dit proefschrift hoofdstuk 2.

II

De conclusie van Klanberg en Spandau dat In_2S een instabiele verbinding zou zijn is niet in tegenspraak met de door Klemm en von Vogel gepubliceerde röntgendiagrammen.

F. Klanberg and H. Spandau, J. Inorg. Nucl. Chem. vol. 19, 180, 1961.
W. Klemm und H.U. von Vogel, Z. anorg. u. allgem. Chem. Bd. 219, 45, 1934.

III

De suggestie van Ross en Bourgon dat GeS een incongruent smeltpunt zou hebben bij 650°C, wordt niet voldoende door hun experimenten gesteund.

L. Ross and M. Bourgon, Canad. Journ. of Chem. vol. 46, 2464, 1968.

IV

Het door Fivaz en Mooser gevonden effect van de groeitijd op het teken van de geleiding van GaSe-kristallen, kan toegeschreven worden aan diffusie van verontreinigingen vanuit de ampulwand.

R. Fivaz and E. Mooser, Phys. Rev. vol. 163, 743, 1967.

V

De verontreinigingsgraad van TlSe, zoals die door Guseinov berekend wordt uit het geleidingsvermogen, dient met voorzichtigheid gehanteerd te worden.

G.D. Guseinov et al., Sovj. Phys. Solid State. vol. 4, 885, 1962.

VI

Bij het opnemen van infraroodspectra van coördinatiecomplexen is het noodzakelijk naast de pellet-methode altijd de mull-methode te gebruiken.

H.B. Jonassen and J.E. Field, J.A.C.S. vol. 79, 1275, 1957.
F.A. Cotton, Modern Coordination Chemistry, Interscience Publishers Inc. New York, 1964.

VII

De gevolgtrekking van Palczewska en Ratajczykowa dat bij hun experimenten waterstof in ijzer penetreert als proton, is aanvechtbaar.

W. Palczewska and I. Ratajczykowa, Bull. Acad. Polon. Sci. vol. 14, 673, 1966.

VIII

Het is gewenst de door Barry en Lay gesuggereerde positie voor het Mn^{2+}-ion in lanthaan bevattend Linde zeoliet X, met behulp van röntgen-analyse nader te onderzoeken.

T.I. Barry and L.A. Lay, J. Phys. Chem. Solids vol. 27, 1821, 1966.

IX

Voor zover dit niet in hun studieprogramma voorkomt verdient het aanbeveling voor natuurkundestudenten die vaste-stofonderzoek willen doen, zich vertrouwd te maken met chemisch preparatief werk.

X

De door Prins in Universiteit en Hogeschool voorgestelde promotie procedure past geheel in het huidige streven naar democratisering van het hoger onderwijs en verdient daarom de volle aandacht.

C. Prins, Universiteit en Hogeschool Jaargang 15, no. 3, 199, 1968.